Polymer integration for packaging of implantable sensors

Yiheng Qin [a], Matiar M.R. Howlader [a,*], M. Jamal Deen [a], Yaser M. Haddara [a], P. Ravi Selvaganapathy [b]

[a] Department of Electrical and Computer Engineering, McMaster University, 1280 Main Street West, Hamilton, ON, Canada L8S 4K1
[b] Department of Mechanical Engineering, McMaster University, 1280 Main Street West, Hamilton, ON, Canada L8S 4L7, Canada

ARTICLE INFO

ABSTRACT

Inexpensive, easy-to-process, light-weight polymer-based materials that are biocompatible, mechanically flexible, and optically transparent have emerged as alternatives to metals and ceramics in the packaging of implantable sensors. These materials have been used to package components such as microelectrode arrays, telemetric coils and structural membranes. Polymers are also being used for the encapsulations and coatings of the implants. The devices and packages require fine-pitch, low-loss, and highly-conductive paths on mechanically and chemically reliable polymer films. In this review, several polymers used for implantation and related integration technologies are identified. We give an overview of novel applications of polymers in implantable sensor packages, and identify future directions for their application. Polymers exhibit high moisture absorption rate, high-frequency electrical loss, and low mechanical stability. These properties are aggravated when polymers are used for *in vivo* applications. Also, the integration of polymers with polymers/metals at high bonding temperatures and pressures may degrade their properties and interfaces. Furthermore, adhesive bonding and physical/chemical deposition methods for the integration may introduce non-hermetic, permeable, optically opaque, and poorly conductive interfaces. Thus, creating polymer-based high-density and small-dimension structures are critical for packaging. To address these issues, polymers with improved characteristics as well as integration techniques using low bonding temperature and pressure are indispensable. Liquid crystal polymer (LCP) and surface activated bonding (SAB) technologies meet these requirements. SAB technologies enable nanoscaled polymer–polymer/metal bonding to realize reliable, miniaturized, and high-performance packages for implantable sensors. This article is meant to serve as a reference for future research in the emerging field of implantable sensors by critically assessing the specific merits and drawbacks of several material-process combinations.

© 2014 Elsevier B.V. All rights reserved.

1. Introduction

For decades, implantable electronic devices have been used in healthcare applications to restore body functions, improve individuals' quality of life, and even save lives [1]. Many implantable devices, such as pacemakers, cardiac defibrillators, artificial cochlear implants, artificial vision prostheses, and neuromuscular stimulators contain complex functional components [2]. These electronic components are not capable of functioning reliably in the warm, moist, and mobile environment of the human body [1]. Thus, effective packages are required to provide a suitable environment for the implants. The quality and reliability of these packages strongly depends on the materials used as well as the integration and bonding of diverse materials and components. Therefore, knowledge of current state-of-the-art materials and technologies is required in order to develop reliable and high-performance implantable devices.

The packages for implantable sensors have to be biocompatible, hermetic and should not outgas. If gas/liquid/moisture penetrates the encapsulant, it may result in device failure [3–5]. These challenges cannot be fully addressed by existing technologies for *in vivo* applications [2]. Therefore, advanced packaging materials and technologies need to be developed to ensure the device reliability and performance. Currently, different metals including titanium

Table 1
A brief comparison of properties among metal, ceramic, and polymer used in implantable applications.

Properties	Metal	Ceramic	Polymer
Biocompatibility	Good for limited metals	Good for bioceramics	Good for many polymers
Hermeticity	Good	Medium	Mostly poor
Degree of outgassing	Low	Low	Mostly high
Mechanical flexibility	Poor	Poor	Good
Reliability	Good	Good	Mostly poor
Optical transparency	Poor	Mostly poor	Good
RF transparency	Poor	Good	Good
Ease of processing	Difficult	Difficult	Easy
Cost	High	High	Low
Relative weight	Heavy	Medium	Light

(Ti), iridium (Ir), platinum (Pt), tantalum (Ta), and their alloys are being used for packaging of implantable pacemakers due to their hermeticity and biocompatibility [6]. Hermetic seals for electrical feedthroughs are employed in these packages as well to avoid unwanted leakage.

The integration of wireless components is another challenge in many implantable sensors with metal packages [2]. When radio frequency (RF) [7] communication is needed in the device, the power-receiving coil or antenna has to be placed outside the metal package, thus increasing the volume of the implant. This requirement is critical because the metal package walls reduce the power transmitting efficiency due to RF signal blockage.

As an RF transparent substitute, bioceramics [8–11] such as aluminum (Al) oxide have been used as the main package materials for implantable devices [12–14]. With the development of more complex implants [15–18], such as retinal implants for blindness and paralysis, smaller implantable electronics with a larger number of input/output (I/O) pins create challenges for traditional techniques like ceramic sintering, as well as metal molding and welding. Although metal and ceramic materials could guarantee long device lifetime, they possess further limitations in terms of miniaturization, I/O densification, mechanical flexibility and high cost, which prevents future mass applications of these kinds of implantable devices. In addition, the hard surfaces of ceramic and metallic packages can introduce unwanted side effects, such as bleeding [19], to the host of the implanted device.

To address the challenges and limitations in metal- and ceramic-based implants, polymeric materials offer the possibility of realizing biocompatible, light, tiny, bendable, and cheap implants with dense I/Os. Candidate polymers include epoxy [20,21], silicone [22], polyurethane (PU) [23], polyimide (PI) [24], poly(p-xylylene) (parylene) [25,26], polydimethylsiloxane (PDMS) [27], as well as the recently developed high-performance liquid crystal polymer (LCP) [28–30]. Their chemical and physical properties offer a number of advantages [31]: (1) some of them are resistant to biological reactions in the human body; (2) their relatively low density reduces the weight of implants; (3) the ease of molding or processing these polymers enables the fabrication of smaller implants with a larger number of I/Os; (4) their increased mechanical flexibility assists in the homogenous joining of human tissues/organs/structures with implants; (5) their ease of combination with other nanomaterials enhances the implants' functional characteristics; and (6) their low cost cuts down on the prices of implantable devices. A concise comparison among metal, ceramic and polymer used in implantable applications is summarized in Table 1. Table 2 lists six important polymers for implantable applications: PI, polyvinyledenedifluoride (PVDF), polyetheretherketone (PEEK), PDMS, parylene, and LCP, as well as some of their properties. These materials will be introduced sequentially in Section 2.

Although polymers possess many unique properties, their integration differs from conventional semiconductor processes due to their varying durability under conditions of high temperature, large external pressure, and the application of chemicals. Table 3 summarizes several integration technologies for polymer–polymer/metal systems, including thermocompression and fusion bonding, direct deposition, agent-mediated bonding and surface activated bonding (SAB). These technologies will be discussed in Section 3. Among them, the SAB technologies have been developed to directly bond smooth surfaces of similar or dissimilar materials. This integration method does not require as much pressure and heat as other methods do, and no thick intermediate material is needed either. Thus, mechanically-, thermally-, and chemically-induced material/performance degradation risks can be avoided. High adhesion strength between bonded pairs, attributable to the atomic forces of the activated surfaces, has been reported using this method [32].

In relevant research domains, a number of review papers have been published. Ghane-Motlagh et al. [33,34] have reviewed the design and implementation of implantable microelectrode arrays. Pang et al. [35] have provided an overview of recent achievements in active sensing units using polymers, focusing on wearable and implantable applications. Hassler et al. [31] have reviewed the properties and applications of five different polymer materials for neural implants. Venkatraman et al. [36] have described the technological progress of implantable cardiovascular polymers. Ramakrishna et al. [37] have presented applications of polymer composites in biomedical science and engineering. Luo [38] and Xia et al. [39] have recently conducted a review of conductive, polymer-based biological research and its applications. Lyu et al. [40] have carried out a comprehensive study on the reliability of polymers in biomedical implants. Jiang et al. [2] have summarized the non-polymer based packaging technologies for implantable devices. So far, there has not been a review of the range of applications of polymer–polymer/metal integration and packaging technologies for implantable devices.

This review examines alternative perspectives on the application of integration technologies of polymers for structural and packaging components in implantable sensors. In Section 2, the characteristics of six polymers for implantable applications are summarized. They are PI, PVDF, PEEK, PDMS, parylene and LCP. Their implantation-related mechanical, electrical and biomedical features are comparatively investigated. In Section 3, the polymer–polymer/metal integration technologies are reviewed. From Sections 3.1–3.4, fusion and thermocompression bonding, laser-assisted bonding, intermediate layer bonding and direct deposition are described as conventional approaches. In Section 3.5, the novel SAB technologies are highlighted. Conventional and novel approaches are compared in terms of their processing parameters, as well as the resulting features. In Section 4, the functions of polymers are categorized into substrates, structural components, and the encapsulants and coatings of the implants. The challenges associating with the application of implantable microelectrode arrays, pressure and biomedical sensors, telemetric structures, and integral systems are presented. Finally, in Section 5, conclusions and perspectives are provided.

Table 2
Properties of six polymers for implantable applications.

Materials	Density [g/cm³]	Glass transition temperature [°C]	Coefficient of thermal expansion (CTE) [ppm/K]	Tensile strength [MPa]	Young's modulus [MPa]	Moisture absorption [%]	Dielectric constant (frequency, [Hz])	USP class	Application challenges	References
PI	1.06–1.45	290–430	3–60	80–392	1800–15,000	2–4	3.5–4 (1k)	–	High moisture uptake, short of rigidity	[41–59,86,361–364]
PVDF	Around 1.78	>−35	120–145	20–50	2000–4000	0.04–0.05	6–10 (1k–1M)	VI	High cost, poor adhesion to other materials, low thermal stability	[74,86,365–370]
PEEK	1.265–1.4	~143	48–58	70–100	3600–3950	0.1	3.1–3.6 (50–50k)	VI	High cost, postoperative infection risk, poor adhesion to other materials	[86–102,371–374]
PDMS	0.95–1.08	−125	180–450	2.24–6.2	0.36–0.87	0.1–1.3	2.3–10.8 (0.1–10k)	VI	High permeability to gases, protein adsorption, limited high frequency electrical property	[86,118–121,375–378]
Parylene	0.71–1.29	35–80: type C 286: type N	35	25–69	0.6–4	0.06–0.1	2.17–3.15 (60–1M)	VI	Fragile, low mechanical strength, poor adhesion to metals	[86,297,379,380]
LCP	1.38–1.95	82–280	4–38	52.8–185	5000–20,000	0.02–0.04	2.8–3.2 (0.5–110G)	VI	Poor adhesion to metal, limited patterning technique	[173–175,177–179, 181–184,186,381]

Table 3
Key features of six polymer–polymer/metal integration approaches.

Integration approaches	Process parameters			Resulting features						Advantages	Process challenges	References
	Temperature (T)	Pressure (P)	Process time	Extra agent	Biocompatibility	Bond strength	Hermeticity	Alignment accuracy	Interface quality			
Fusion and ther-mocompression bonding	High	High	Long	No	Good	Strong	Good	Poor	Degradation of heated materials	Easy imple-mentation	High T & P required	[28,29,176,188,190, 191,201–203]
Laser assisted bonding	Locally high	Medium	Vary	Laser	Good	Locally strong	–	Medium	Degradation of heated materials	Arbitrary bonding pattern	Laser required	[212–222]
Intermediate layer bonding	Medium	Medium	Medium	Adhesive, solvent	Medium	Medium	Poor	Poor	Interface with extra materials	Reduced T & P, allow more material combinations	Extra agent required	[25,26,223–231, 233–240]
Physical vapor deposition	Vary	0	Vary	No	Good	Vary	Poor	–	Adhesion layer may be needed	Compatible with current processes	Adhesion problem	[201,243–245]
Electrochemical deposition	Low	0	Vary	Electrolyte	Medium	Low	Poor	–	Adhesion layer may be needed	Low T process	Chemical required, film quality	[192,198–200]
Surface activated bonding	Low	Vary	Long	No	Good	Strong	Good	Good	Smooth, no degradation	Refer to Section 3.5	Long process time	[32,187,193–197, 247–260]

2. Polymer materials for packaging of implantable sensors

Most polymers are soft, light, RF-transparent, easy-to-process, and low-cost. Many of them can potentially address the challenges associated with metals and ceramics for implantable applications. Table 2 shows the corresponding properties of six important implantable polymers: PI, PVDF, PEEK, PDMS, parylene, and LCP. They are used not only as substrate and structural materials, but also as encapsulants for sensors. These polymers meet the basic criteria for use as implantable packaging materials. They have high resistance to chemical reactions in the biomedical surroundings, high mechanical strength, and high mechanical compatibility with biological tissues. This section will briefly review the potential, as well as the challenges, of using these polymers as structural and packaging materials for implantable sensors.

2.1. Polyimide

Polyimide materials are polymers made of imide monomers that have been used in a wide range of electronic applications. They have high electrical resistivity of over 10^{16} Ω cm and dielectric strength of 2×10^{16} V/cm [41]. They also exhibit a relative dielectric constant between 3.5 and 4 around 1 kHz [42]. These properties are similar to silicon (Si) based insulating materials such as SiO_2 and Si_3N_4. PIs are also low-cost materials that have low density, high mechanical reliability, high thermal stability, and mechanical flexibility [42–44]. Because of their promising mechanical properties, PIs are widely used for fabricating flexible cables and medical tubing, as well as for fabricating insulation and passivation layers in integrated circuit (IC) and micro-electro-mechanical system (MEMS) chips [42].

Besides these properties, the diversity in chemical compositions and additives offers PIs a wide range of applications: (1) Pyralin PI2723, which can absorb moisture more effectively, can be used in moisture sensors [45,46]; (2) owing to its magnetic characteristics, Dupont PI2555 has been applied in magnetic micro-actuators [47,48]; (3) a temperature sensor has been realized by Dupont PI273 [49]; and (4) shear stress sensor arrays have been built using Dupont PI2808 because of its high tensile strength [50]. Some PIs have high chemical resistivity [51] and biosafety [52] properties due to the tight and close arrangement of their molecules [53]. The chemical stability of PIs makes them reliable insulation materials on gold (Au), Al, and Ti films in the human body at 37 °C [52,54]. Thus, in the last few decades, PIs have been applied in biomedical applications as reliable substrates, coatings, and insulators [55–59].

Although the mechanical flexibility of PI is attractive for implants, it easily buckles during implantation due to its lack of stiffness [60]. This property reduces the accuracy of the implant's position. In addition, the long-term device reliability of PI-based implantable electronics has seldom been reported. Attention should be paid towards preventing moisture-induced material degradation of PI based sensors in the human body [61].

2.2. Polyvinyledenedifluoride

PVDF is a chemically stable thermoplastic fluoropolymer synthesized by the polymerization of vinylidene difluoride. The semi-crystalline piezoelectric PVDF polymer has four phases: α, β, γ and δ. The β phase PVDF possesses the largest effective dipole moment [62] and can be utilized for pressure sensing applications. As early as 1969 [63], PVDF's coefficient of piezoelectricity was measured to be 6 to 7 pC/N, at least one order of magnitude greater than that of other polymers at that time. To enhance the material's piezoelectricity, PVDF-based copolymers are synthesized to improve material crystallinity, although the degree of polarization of the unit structure might be reduced. One common PVDF copolymer is poly[(vinylidenefluoride-*co*-trifluoroethylene])

(PVDF-TrFE), which has a piezoelectric coefficient of 38 pC/N [64]. The thermal, mechanical, and electrical characteristics listed in Table 2 make PVDF suitable for sensor [65–68] and energy harvesting applications [69–72].

Like many other fluorocarbon polymers, PVDF is chemically inert. Its high resistance to hydrolysis, low degradation rate, and aging-independent material stiffness reveals the material's biocompatibility [73] (U.S. Pharmacopeial (USP) class VI [74]). When PVDF comes into contact with human tissue, minimal cellular response without mineralization, intimal hyperplasia, or excessive fibrous tissue reaction has been detected [75]. Thus, PVDF can be used as packaging material in implantable devices, as well as active sensing structures due to its piezoelectricity. Its biomedical applications include, but are not limited to, surgical meshes [76–78], vascular sutures [75,79–81], and implantable pressure sensors [82,83].

The non-reactive property of PVDF causes poor adhesion to other materials [84]. Other drawbacks of this material include: (1) its inability to form smooth films [84]; (2) its relatively low thermal stability (upper limit of 80 °C) due to its low glass transition temperature (T_g) [85]; (3) its large vibration of relative dielectric constant (6–10) in the frequency range from 1 kHz to 1 MHz [86]; and (4) its high cost (especially of the PVDF-TrFE copolymer).

2.3. Polyetheretherketone

PEEK is a semi-crystalline polymer consisting of monomers of two ether groups and a ketone group. PEEK and its composites exhibit excellent mechanical [87–94], thermal [95–97] and chemical [98–100] properties. They have high mechanical strength and stiffness, good fracture toughness, compatibility with many sterilization techniques, high corrosion resistivity, and are easy to process by molding or machining. Also, the density of PEEK is 1.32 g/cm, which is comparable with the density of human bones and muscles [101,102]. The relative dielectric constant of PEEK stays stable between 3.1 and 3.6 when the frequency sweeps from 50 Hz to 50 kHz [86]. Numerous studies [103–107] have shown that PEEK can be used for clinical applications, since it can serve as a substitute for Ti/Ti alloys in biomedical implants [108–112].

Carbon fiber-reinforced PEEK has enhanced performance for fracture fixation [113]. The flexural fatigue properties and thermoformability of polystyrene, polybutylene terephthalate and 30% chopped polyacrylonitrile carbon fiber-reinforced PEEK has been studied. PEEK exhibited the highest fracture toughness and bending fatigue resistance due to its compatibility with carbon fibers. Also, it was insensitive to preconditioning and thermoforming.

The drawbacks of PEEK are its high cost and its dimensional instability [114], which prevents widespread application. As a packaging material, its low surface energy may result in weak bonding with other materials using conventional adhesives [115]. In addition, there are risks for postoperative infections if PEEK is implanted in the human body [116].

2.4. Polydimethylsiloxane

The PDMS elastomer, a silicone polymer that has a backbone of silicon-oxygen linked with methyl groups, is formed by crosslinking polymeric chains [117]. The strength, durability [118], flexibility [119], and wide-range-usage [119] of PDMS are attributable to its physical and chemical properties, including: (1) its low Young's modulus of 1 MPa [120]; (2) its low shear modulus of between 100 kPa and 3 MPa [119]; (3) its low T_g around −125 °C [119]; (4) its high dielectric strength around 14 MV/m [121]; (5) its low chemical reactivity; and (6) its non-toxicity [121]. Another advantage of using PDMS in electronic industries has to do with its low-cost process compatibility. PDMS can be spin-coated onto substrates to

form thin films, or it can be molded to form different geometries [122]. To improve its flexibility in processing, a photo-definable PDMS has been developed. Although photo-definable PDMS is still not suitable for biocompatible components [31], other implantable PDMS materials may easily be patterned by wet or dry etching [123–125].

In biomedical applications, non-photo-definable PDMS has been used widely as an encapsulant for long term implants and has obtained a USP class VI certification [126]. Early experiments in the 1970s demonstrated that PDMS was stable for approximately 25 years in the human body [127]. Another study demonstrated that the chemical properties of PDMS remained unchanged after over two years of implantation [128]. All the aforementioned characteristics make PDMS attractive for biomedical applications such as artificial organs and tissues due to its compatible stiffness [129–132]. As well, its chemical stability allows it to be used in biomedical microfluidic components [133–137] and sensors [27,138–142], drug delivery systems [143,144], and certain biocompatible coatings [145,146].

PDMS has high gas permeability [31], which prevents it from being used as hermetic packaging material for long-term implantable devices (such as implantable neural microelectrodes). As well, when PDMS surfaces are exposed to biofluids, protein adsorption presents a challenge for biomedical applications [147]. Moreover, the electrical performance of PDMS is not ideal [148]. Its dielectric constant varies from 2.3 to 3.8 within the frequency range of 0 to 50 Hz. As a result, it is not suitable for use as the substrate of telemetric structures.

2.5. Poly(p-xylylene)

In the poly(p-xylylene) polymer family, parylene-C (one chlorine in the monomer structure) is used in implantable devices because of its good electrical and chemical barrier properties [149,150], dielectric performance [151], and chemical and biological stability [152,153]. Normally, parylene-C is polymerized *via* vapor deposition process, leading to thin, conformal, and pinhole-free films with low intrinsic stress [153–156]. This promising material has been utilized in microwire coatings [157], micromachined Si electrode arrays [158], as well as the packaging of microfluidic devices [159], retinal stimulation arrays [160,161], and flexible nerve cuffs [162].

Similar to parylene-C, parylene-D has two chlorine groups in the monomer structure and a higher density than parylene-C [163]. Thus, this material is a better barrier to prevent moisture diffusion. However, the poor uniformity of the film limits its applications [163]. Both parylene-C and parylene-D are derivatives of parylene-N, which has no chlorine group in its chemical structure and is manufactured from the *p*-xylylene intermediate [163]. As a type of newly-developed parylene polymer, parylene-HT not only has features of conventional parylenes (type N, C and D), but also has superior thermal stability (up to 450 °C) and good dielectric properties (dielectric constant is between 2.2 and 3.2 through 60 Hz to 1 MHz) [164]. The variation of the dielectric constant changes the performance of the device when working at different frequency ranges. This effect can be observed in both neural signal recording at several kHz and wireless communication at higher frequencies. An additional type of parylene is called "reactive parylene," which has reactive functional groups linked on the polymer main chains, and chemical reactions can happen between reactive parylene and other chemicals in certain conditions [165–167].

Except for these advantages, parylene still has several shortcomings: (1) it has low mechanical strength which makes it difficult to handle [31]; (2) it has weak adhesion to metal surfaces; (3) it exhibits poor stability under long-term saline soak; (4) it suffers from stress cracking due to high currents in devices [168–170];

and (5) it has a relatively high moisture absorption rate. These challenges limit its applications in implantable devices [171].

2.6. Liquid crystal polymer

The moisture from the human body will eventually pass through the packages of implanted electronic components and affect their operation. Moisture-generated surface ions may cause reliability issues such as electrical short circuits and/or component degradation, and subsequently may result in the failure of the device [172]. Compared with other polymers like PI (moisture absorption of 2–4% [86]) and parylene-C (moisture absorption of 0.06–0.1% [86]), the newly-developed thermoplastic LCP material has a much lower moisture absorption rate (less than 0.04%) [173,174]. Moreover, the gas permeability of LCP is not affected by increasing the environmental humidity or the surrounding temperature (*e.g.* till 150 °C) [175]. Thus, the application of LCP could possibly ensure much higher long-term reliability of implanted devices.

If implantable devices require wireless communication [176], the high frequency electrical performance of the packaging components, such as the substrate, is extremely essential. Results have shown that LCP has a low and constant relative dielectric constant around 3 from 0.5 to 110 GHz and a low loss factor of 0.002 to 0.0045 up to 100 GHz [177–179]. It has also been reported that LCP packaging of monolithic microwave ICs had almost no influence on the RF performances of the devices [180]. The high frequency characteristics of LCP are superior to other polymeric materials.

Because of LCP's considerable heat resistance, small CTE value, high chemical resistance, high mechanical flexibility, promising biocompatibility, and low cost (50% to 80% lower than Kapton® PI film) [173,181–184], it has been used for high-density printed circuit boards [175,185] and semiconductor packaging [186]. In addition, the low moisture uptake and stable dielectric constant over a wide frequency range makes LCP a promising substrate and packaging material for *in vivo* applications.

While LCP has superior characteristics, the poor adhesion between LCP and metals is a critical barrier for implantable applications [187]. Another challenge is the difficulty of making patterns on LCP. Unlike some other polymers, LCP is not photo-patternable. However, structures in LCP can be formed by laser-machining or reactive ion etching (RIE) [31]. Therefore, LCP may be used in biomedical applications.

3. Polymer integration technologies for implantable sensors

Section 2 identified the suitability of polymer materials as substrates, structural components, and encapsulants for the packaging of implantable electronics. However, many implantable devices require the integration of two or more dissimilar materials. For instance, a metal film and a polymer layer need to be bonded to form flexible and durable electrical pathways in order to form electrical interconnections; a polymer coating should be deposited on some metal components to prevent *in vivo* electrochemical corrosion. Thus, the integration of metal structures with polymer films becomes one of the most critical steps in the fabrication of implantable devices.

Several criteria for assessing the integration quality of the implantable metal-polymer systems have been proposed [32]. Integration quality is mainly related to the performance of the integrated interface, and the associated challenges include, but are not limited to: (1) the weak bond strength; (2) the low electrical conductivity; (3) the low hermeticity of the seal; (4) the low alignment accuracy; (5) the poor optical transparency; and (6) the poor biocompatibility due to foreign materials across the bonded interface.

First, the high bond strength ensures the mechanical stability and reliability of metal-polymer systems in an actively moving human body. Second, the high electrical conductivity reduces the energy loss in the electronic components. The high frequency conductivity of metal films may dominate the transfer properties of RF signals when wireless communication is required. Third, a hermetic seal provides a suitable dry and chemical-free environment for critical components, thus prolonging the life of the device. Fourth, high alignment accuracy is required for the miniaturization of devices with high-density structures such as retinal implants. As well, in devices such as retinal implants, high interface optical transparency directly reduces the reflection of incident light, improving device performance [32].

In this section, several polymer-related integration approaches will be reviewed based on the material properties mentioned in Section 2. The LCP is mainly reviewed here because of its superior behaviour over other polymers. Technical challenges in conventional processes will be addressed, and novel surface activated bonding/laminating technologies for future nanointegration will be emphasized. Table 3 summarizes the key features of six polymer–polymer/metal integration approaches.

3.1. Fusion and thermocompression bonding

Both fusion and thermocompression bonding are direct bonding techniques. In these methods, the objective is to melt or increase the diffusion rate of at least one of the atomic-contacted materials to create bonds at the interface. Both fusion and thermocompression bonding processes require treatments at an elevated temperature for enhanced interfacial adhesion between polymer and polymer/metal. The difference between fusion and thermocompression bonding is that thermocompression would require a relatively lower temperature than fusion bonding, but much higher external pressure applied at the bonding site. The purpose of using higher external pressure is to ensure atomic contact between the material surfaces. In conventional integration technologies, one typical example is to bond copper (Cu) through silicon vias to Cu bumps [188]. In recent research, fusion bonding and thermocompression bonding have also been utilized in implanted electronics due to their ease of implementation and the need for less sophisticated equipment.

While fabricating an LCP-based implantable planar coil, Jeong et al. [176] used two types of LCPs with different melting points. Cu foil was first cladded on both sides of high-temperature LCP and patterned. Then, thermocompression bonding was carried out at 285 °C—above the melting temperature of low-temperature LCP (280 °C), but below that of high-temperature LCP (325 °C), in order to melt the low-temperature LCP layer in-between. The melted low-temperature LCP acted as the adhesion layer between two high-temperature LCP layers, filling the gaps between the inner Cu wires and forming the coil encapsulant. The gas-impermeable LCP protected the Cu wires from degradation, and promising RF performance was realized. Note that Cu is an unsafe material in some implantable applications. For example, Cu in the eyes can cause chalchosis bulbi [189].

However, the feasibility of incorporating Cu with various polymers has been investigated using different integration technologies [28,29,190–200]. Sundaram et al. [29] have reported a novel LCP–Cu fusion bonding process to realize fine pitch interconnections for retinal and neural prosthetic applications. Its fabrication and integration process is described as follows: Cu foil was first patterned and treated with a thin layer of palladium (Pd). The patterned Cu foil was then laminated with 50 μm thick LCP at 288 °C with 0.69 to 2.07 MPa applied pressure that lasted for 45 to 60 min. The high lamination temperature made the LCP flow in between the patterned Cu foil template, creating a strong bond between Cu

and LCP. The resulting interconnections displayed high adhesion strength and biocompatibility. The interface leakage rate was lower than 5×10^{-13} Pa m^3/s.

Apart from LCP, parylene to parylene thermocompression bonding has also been employed at 230 °C for 30 min with an applied force of 3000 kg m/s^2 to fabricate flexible structures [201,202]. Chen et al. [203] have presented a "fold-and-bond" approach to fabricate inductor coils with enhanced quality factors on parylene-C substrates for implantable applications. The basic principle of this development was to increase the thickness of planar metal coil by folding and bonding two symmetric thin coils that were initially manufactured on the flexible substrate. The bonding step was carried out at 250 °C for 24 h. Results showed that the quality factor of the fabricated planar coil almost doubled, but the misalignment between the two thin coils was as large as 10 to 20 μm.

The disadvantage of thermal-assisted bonding technology is the requirement of high temperature and, sometimes, high external pressure [204–211]. These processing conditions degrade polymers and reduce the alignment accuracy. In the applications requiring small-dimension and high-density structures, the alignment of fine structures on polymers will be rather difficult using high temperature processes. This is due to the relatively large CTE values of polymers, which are incompatible with those of rigid inorganic materials.

3.2. Laser-assisted bonding

Laser-assisted bonding involves photochemical reactions. The reactions alter the chemical compositions of the materials at the bonded interfaces where the chemical bonds are formed [212,213]. In this technique, the materials to be bonded include an absorbing material and a transparent material [214,215]. The laser beam is absorbed by the absorbing material after penetrating the transparent material, resulting in heat at their interface. The temperature at the interface goes beyond the melting point of one material, and the energy is sufficient to create chemical bonds between the two materials.

This technique has been demonstrated by Wang et al. [216], using a 100 μm thick polyethylene terephthalate (PET) film bonded with a 100 μm thick Ti foil for the packaging of implantable devices such as pacemakers. In this case, a near-infrared diode laser was used to bond the materials. The bond strengths of the interfaces varied from 65.46 to 90 MPa. The bond strengths were attributed to the laser induced Ti—carbon (C) bonds in the interfacial region. In addition, Georgiev et al. [213,217–219] developed a similar process for the bonding of different materials. Both Kapton® FN PI film and Teflon® fluorinated ethylene propylene film were bonded with Ti film using laser-assisted bonding. The measured bond strengths of the two types of samples were 3.32 MPa and 8.48 MPa, respectively. It was found that the laser-induced Ti—F bonds mainly contribute to the bond strengths.

In some circumstances, one transparent polymer has to be bonded with another piece of transparent polymer film or a glass lid (for example, the substrate and encapsulant of the intraocular implants need to be transparent). Potente et al. [220], Ebert [221], and Kim and Xu [222] have demonstrated PI/PET-glass micro pump structures using laser-assisted bonding. Process parameters, such as laser power, focal length of the lenses, and exposure time, were controlled to introduce heat to the interface of two transparent materials by laser.

Compared with thermocompression and fusion bonding, laser-assisted bonding can preserve the material properties due to the localization of heat at the bonded region. An arbitrarily shaped bonding region can be achieved using a laser beam. Nevertheless, the applicable materials are limited in this technique, since there

must be one transparent material and one absorbing material. The scope of this process is also limited by its low processing yield.

3.3. Bonding with intermediate layer

Two different materials cannot be directly bonded together easily due to bonding constraints produced by high temperatures and surface wetting conditions. Hence, alternative approaches to achieve a reliable bond, based on intermediate layer assisted bonding, have been explored. These approaches include adhesive bonding and solvent-assisted bonding.

3.3.1. Adhesive bonding

Adhesive bonding is a technique of joining two or more similar or dissimilar materials using adhesive layers. The adhesive layers can be cured using either heat [223,224] or ultraviolet (UV) treatments [225–228]. UV treatments have been more commonly used. Adhesive bonding of polymethylmethacrylate (PMMA) has been demonstrated in fabricating microfluidic devices using PDMS [226], SU-8 photoresist [229], and prepolymerized methyl methacrylate [230,231]. The use of some adhesives (such as reactive parylene) also results in chemically-induced covalent bonds [25,26]. Parylene-C layers laminated with complementary poly(p-xylylene)-amine (PPX-CH$_2$NH$_2$) and poly(p-xylylene)-aldehyde (PPX-CHO) adhesion layers have been demonstrated by Seymour et al. [26] to create hermetic seals over metal electrodes for implantable electronics. When the parylene layers were heated up to 140 °C for 3 h, the joint was formed through carbon–nitrogen (C—N) chemical bonds.

Adhesive bonding offers the possibilities of lowering the bonding temperature and pressure. However, they introduce different materials to the bonding site, which may affect reliability due to their biocompatibility and problems induced by CTE-difference.

3.3.2. Solvent-assisted bonding

Solvent-assisted bonding integrates materials below their T_g using solvent films. In this method, no adhesive is required and no different material will be left at the bonded interface. However, the temporarily applied intermediate solvent film causes swelling of polymers and softens their surfaces [232]. Thus, the mobility of polymer molecules increases. A joint diffusion zone between the polymers is formed once external pressure is applied. With the evaporation of the solvent, the bonding interface is created. Solvent-assisted bonding has potential as a mass fabrication process with high throughput [233], since solvent may be deposited to the surfaces of polymers either in liquid or vapor phase. Solvents that have been used for fabricating microfluidic devices made from PMMA include: acetonitrile [234,235]; ethanol [236]; isopropanol [237]; low azeotropic solvent consisting of 1,2-dichlorethane and ethanol [238]; ethylene glycol dimethacrylate [239]; as well as a mixture of dimethyl sulfoxide, water, and methanol [240].

The introduction of an intermediate layer compensates for CTE mismatch at the bonding interface, and thus allows for a variety of material combinations. It also assists with bonding by reducing the applied temperature and pressure. However, there are some critical issues with this technology, including reduced biocompatibility and poor hermeticity caused by the intermediate layer. In general, the intermediate layers are polymer materials that cannot guarantee the hermeticity. They also affect the reliability of the bonded interfaces.

3.4. Direct deposition

Since the direct deposition of thin films of metals and other materials have been extensively studied [241], in this section we will review approaches for metal deposition on LCP substrate,

which is an excellent polymeric material for biomedical applications. Deposition methods of metal on LCP include physical vapor deposition (PVD) as well as electroless and electrolytic deposition.

3.4.1. Physical vapor deposition

PVD is achieved through the use of evaporation and sputtering techniques [242]. These techniques are widely used in semiconductor and MEMS industries due to their technological maturity and the feasibility of batch processing. For polymeric implantable bioelectronics, electron-beam evaporated Pt, Au, and Ti on LCP substrates have been studied by Howlader et al. [243,244]. This study focused on the conductivity, stability and charge delivery capacity (CDC) of the metal films to avoid irreversible Faradaic reactions. The results suggest that the surface roughness of the substrate and metal, as well as the reactivity and capacitance of the electrode, affect the impedance and long-term electrochemical stability of metal films. In comparison to Ti and Au, Pt electrodes offer lower impedance at neuromuscular stimulation frequencies (1–250 Hz), and a higher CDC. However, Pt and Ti were less stable than Au electrodes.

On the other hand, Ha et al. [201] have reported that a sputtered Ti/Au bilayer can be integrated between or on LCP and parylene films. The metals behave as the electrodes of a capacitive pressure sensor for intraocular pressure monitoring. Also, iridium oxide (IrO$_2$) sputtered films have been studied for flexible nerve stimulation electrodes due to IrO$_2$'s superior charge injection capability [245].

The challenge in using this technique is the poor adhesion of the polymers with deposited materials. This challenge can be addressed by matching the surface energies between the metals and the polymers. Surface energies can be matched by treatment of material surfaces, or by adding adhesion layers. However, the flatness and transparency of the bonded interfaces is sacrificed.

3.4.2. Electroless and electrolytic deposition

Chemical reduction reactions in electrolytic and electroless deposition occur in an aqueous solution with and without the use of external electrical power. As mentioned, the poor adhesion between the substrate (such as LCP) and the deposited metal (such as Cu) is one of the critical issues in the integration of implantable electronics. Generally, the adhesion between the polymer and the metal is achieved by either mechanical interlocking or chemical bond formation between the modified surfaces [192]. As a result, both wet chemical treatment and dry treatment (plasma treatment and RIE) are usually employed to modify the LCP surfaces to allow for improved adhesion [198,200]. Moreover, since the electroless deposition has difficulty in forming thick metal layers, it is recommended to combine the electroless and electrolytic deposition processes for practical applications.

Chen et al. [198] have developed a Cu deposition process on LCP. This process consists of the wet chemical modification of the LCP surface, the surface treatment with a Pd catalyst layer, the electroless deposition of 5 μm thick Cu, heat treatment, and, finally, Cu electroplating. This process allows for the fabrication of metal films as thick as 40 μm. Typically, the adhesion strength of Cu film on LCP was 0.54 MPa. Based on this process, M. Zhou et al. [199] studied the aspects that would affect the adhesion strength between plated Cu and LCP substrate. Results showed that potassium permanganate was an effective chemical for surface treatment because it could introduce hydrophilic groups on the LCP surface. The optimized etching time was 20 min, achieving the adhesion strength of 12.08 MPa.

Finally, Ge et al. [200] compared the adhesion behaviors of electroless-deposited Cu and sputtered Cu on LCP with different pretreatments. The Cu/LCP bonded interface was pulled apart using a tensile pulling tester and the fractured surfaces were examined

using scanning electron microscopy (SEM). Chemically-deposited Cu was delaminated from untreated, plasma-treated, and RIE-treated surfaces. Sputtered Cu was also easily delaminated from chemically-treated LCP surfaces. Both phenomena indicated the failure occurred as a result of a complete adhesive fracture along the Cu/LCP interface. For electroless plated Cu on chemically-treated LCP, thin LCP debris appeared on the backside of Cu film, showing a mixed failure mode of both adhesive and cohesive. In other cases, cohesive failure was identified where the LCP side showed fiber-like morphology, whereas the Cu side showed a ductile deformation of the LCP.

Electrochemical deposition provides a low-temperature polymer–metal integration approach. It allows the deposition of relatively thick metal layers; however, unwanted chemical reactions can introduce impurities in the process solution, affecting the quality and adhesion of the deposited films. As well, the polymer–metal adhesion is influenced by the process-induced stress in soft polymer sheets.

3.5. Surface activated bonding/lamination

The aforementioned polymer-related bonding and integration technologies are sometimes incompatible with certain system integration applications such as implantable electronics due to their demand for high external pressure, elevated temperatures, and chemical solvents. Without such prerequisites, it is difficult to integrate various materials with small dimensional structures. The alignment accuracy or deformation of optical components, such as polymer lenses and delicate MEMS devices, also presents a challenge to the use of conventional integration approaches [246].

To address such challenges, SAB technologies have been developed that are capable of integrating combinations of metals, semiconductors, and insulators at room temperature, or at least a much lower temperature and pressure than the aforementioned processes. So far, SAB has been demonstrated using various combinations of materials including Cu [193–195], Au [194], Si [247–249], *III-V* semiconductors [250–253], ionic materials (for example, LiNbO$_3$) [254–258], and LCP [187,196,197,259].

SAB technologies can be categorized into four groups [32,260]: direct adhesion, nano-layers adhesion; sequential plasma activation; and hybrid adhesion (sequential plasma activation with electrostatic treatment). Their working mechanisms are described in Fig. 1. For the first approach (Fig. 1a), the surfaces of bonding pairs are cleaned with an argon (Ar) fast atom beam, which removes the contaminants such as carbon and oxides. Direct adhesion takes place when the smooth surfaces are attached in an ultra-high vacuum (UHV) at room temperature. High bond strength can be achieved because of the formation of covalent bonds between the pair [247].

Bonding of ionic materials is challenging because their surface activation results in inhomogeneous polarization. In the second approach (Fig. 1b), the polarization issue is addressed by simultaneously activating the surface and depositing a nanoadhesion layer (for example, a few nanometers of iron) [257,258]. This approach enhances the adhesion between the contacting surfaces. High bond strength is obtained spontaneously between the contacting surfaces in low vacuum or UHV.

In the third approach (Fig. 1c), the surfaces are cleaned using RF RIE and microwave-neutral radicals in a low vacuum environment. Bonding is carried out in the controlled air of a class 1000 clean room. The sequential plasma activation produces highly hydrophilic and reactive surfaces. This process generates nanopores as well as oxides on the surfaces. Therefore, the water at the bonded interface is absorbed by the bulk material, resulting in strong covalent bonding at the interface [261].
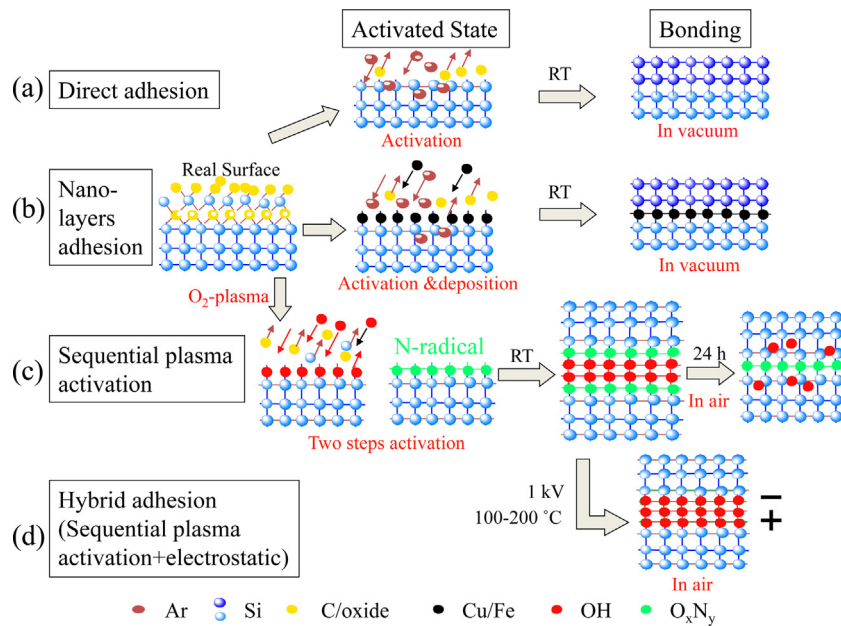
The sequential plasma activated bonding process produces interfacial voids due to the absorbed water in the bulk material. The fourth approach (Fig. 1d) addresses this issue. After using the third approach to bond the wafers, the bonded wafers are post-treated using anodic bonding in the controlled clean room air. This treatment results in a void-free bonded interface with high bond strength. This result is produced by the adhesion between the hydrophilic and reactive surfaces under the application of electrostatic force [262,263].

Generally, activated polymer surfaces with nanoadhesion layers are difficult to bond with metals at room temperature. This low bonding strength is a consequence of the high roughness of the polymer surfaces. Therefore, in the SAB approach, the surfaces of Cu and LCP were first cleaned by Ar-RF plasma etching in a low vacuum environment to remove the surface oxide and contaminants. Then, a Cu nano-layer was deposited onto the LCP, and the bonding was done at room temperature by a roller laminator [196]. Subsequently, the Cu/LCP system was heated in Ar atmosphere outside the bonding chamber at a temperature below the T_g of LCP. This process resulted in a higher bonding strength than that of conventional lamination using heat. Also, the size of samples was no longer constrained to wafer-sizes. Therefore, this process has promising applications for large-area and low-cost production. Fig. 2 shows images of a 210 mm × 297 mm piece of laminated LCP/Cu system (Fig. 2a) prepared by such method, and a peel strength comparison after annealing the system in different gases (Fig. 2b) [187]. The peel strength of the Cu/LCP system was dependent on the annealing gases. The peel strength of samples annealed in Ar and N$_2$ was significantly higher than that of samples annealed in the air or O$_2$. The specimens sequentially annealed in Ar/N$_2$ and O$_2$ showed significant peel strength reduction as the atmosphere was changed.

An x-ray photoelectron spectroscopy study of the delaminated surfaces showed that sputter etching produced an LCP surface with a reduced amount of oxygen [187]. Consequently, the adhesion between Cu and LCP was improved by the following process: the Cu adhesion sites were bonded to the plasma-induced dangling sites on nano-Cu coated LCP, and then thermal reconstruction of nano-Cu layers was achieved by annealing in Ar and N$_2$ gases. This result differed from the mechanical interlocking that is observed in the conventional lamination of polymer–metal systems. While annealing the specimens in the air or O$_2$, the diffused O$_2$ oxidized the deposited Cu along the interfaces, resulting in weak bonding.

The advantages of the enhanced adhesion of SAB Cu/LCP, in terms of its electrical properties, can be demonstrated *via* fine-pitch patterning and measuring the frequency-dependent conduction loss [196,197]. Fig. 3 shows the testing structure of Cu wires of 50 μm width and pitch on LCP, as well as its frequency-conductivity relation with the Cu/LCP interface. In both SAB and conventional laminated systems, the measured conduction loss increases with frequency. However, a three-fold lower loss for the SAB system was observed in comparison to conventionally-laminated specimens (Fig. 3b). The lower conduction loss of the SAB specimens was attributed to their lower interface roughness (64 nm for SAB specimens compared with 970 nm for conventionally-laminated specimens, root-mean-square value). In addition, the influence of high frequencies on the interfacial conductivity of Cu/LCP was examined. 10 μm thick Cu–Zr alloy was bonded to 50 μm thick LCP with 19 nm thick sputtered Cu–Ni alloy in between. The conductivity of the bonded interface remained above 90% at 20 GHz (Fig. 3c). This indicated the potential high frequency applications of metal-polymer systems fabricated by SAB. For the RF antennas in implantable systems for power transmission or communication, high interfacial conductivity could enhance the signal transfer efficiency to improve the system performance, and it could reduce heat generation in order to prevent surrounding tissues and organs from burning.

Fig. 1. Schematic for SAB technologies that provide atomic-level bonding through (a) direct adhesion, (b) nano-layers adhesion, (c) sequential plasma activation, and (d) hybrid adhesion [32].

In summary, the major advantages of the SAB techniques for polymers compared with conventional bonding and integration methods are: (1) the ability to bond low surface energy polymers with high bond strength; (2) the small amount of polymer defects resulting from the application of pressure, heat, and chemicals; (3) the high alignment accuracy between flexible materials resulting from the use of lower temperatures; (4) the biological compatibility of the bonding interfaces due to the minimal use of adhesion layers (nanometers thickness); and (5) the realization of mechanical, electrical, and optical connections on the same bonded interface. However, the long processing time of SAB is its drawback.

4. Applications of polymeric packages in implantable sensors

As discussed, polymers act as the substrates, encapsulants, and/or structural components of the sensors. Also, the nature of the packaging influences the performance, lifespan, and cost of implantable sensors. Although there are challenges remaining in the interdisciplinary areas of materials, electronics, and biomedical technologies, a number of biocompatible polymers have been integrated for the packaging of implantable sensors. Some typical examples include the substrates of microelectrode arrays and telemetric structures, the structural components (*i.e.*, membranes and walls) of pressure and biochemical sensors, and the sealing/coating of implantable devices, as shown in Fig. 4. The details of this system are beyond the scope of this article, and are not shown in this figure. A list of the applications of these different polymers is shown in Table 4.

4.1. Substrate of microelectrode arrays and telemetric structures

Implantable microelectrode arrays interface between biological neural/muscular systems and electronic devices [264], functioning to sense, modulate, and stimulate neural/muscular activities. A typical example of sensing biological signals using microelectrode arrays is the electrocorticogram (ECoG). ECoG surface electrode arrays can provide images of brain activities by probing the cortical surface [265]. A lot of effort has been spent on designing

and fabricating flexible ECoG electrode arrays, from a small sampling area with low electrode density to a large area with high electrode density. In cases such as this, when RF communication is required in implantable devices [266,267], polymeric materials are preferred over metals because of their RF transparency. Many groups have proved the feasibility of using miniaturized inductor-capacitor sensors for wireless sensing in a number of implantable applications, including sensing transcutaneous pressure, intracranial pressure, and pressure resulting from abdominal aortic aneurysms [268–272]. In these applications, PI, PDMS, parylene, and LCP have been widely studied and will be presented in this review paper.

4.1.1. PI substrates

A research group [273,274] has developed a method to fabricate 8×8 flexible electrode arrays on Kapton® PI films, with a $150 \, \mu m$ electrode diameter and $750 \, \mu m$ pitch. The electrode arrays were implanted into rats for signal recording and attained reproducible data over 100 days. Due to the electrodes' small dimensions and close distance to tissues, there was also potential to realize high spatial resolution mapping for the responses evoked by using these devices. Later, Brunner et al. [275] utilized a similar 64-electrode component on PI substrates to set up a real-time functional mapping system for studying the neural mechanisms of visual attention and its directional orientation [276–278]. Patrick et al. [24] have fabricated flexible implantable electrode arrays on PI substrates to process the activities of large ensembles of cortical neurons. The resulting subcutaneous platform reduced overall implant dimensions, and a reliable *in vivo* electrode-*in vitro* electronics interface.

While 64-channel ECoG electrode arrays are commonly studied, it has been found that better ECoG sensors require higher spatial resolution [279], either by adding micro ECoG fill-in or by shrinking electrode pitch to a shorter distance. In order to study the interaction mechanisms between neuronal populations, Rubehn et al. [280] used a micromachined $35 \, mm \times 60 \, mm$ ECoG electrode array consisting of 252 channels on a thin PI substrate, enclosing Pt electrodes and conductive paths. Because of the large amount of electrodes combined with the flexible PI substrate, this device could carry out simultaneous signal recording over several brain areas.
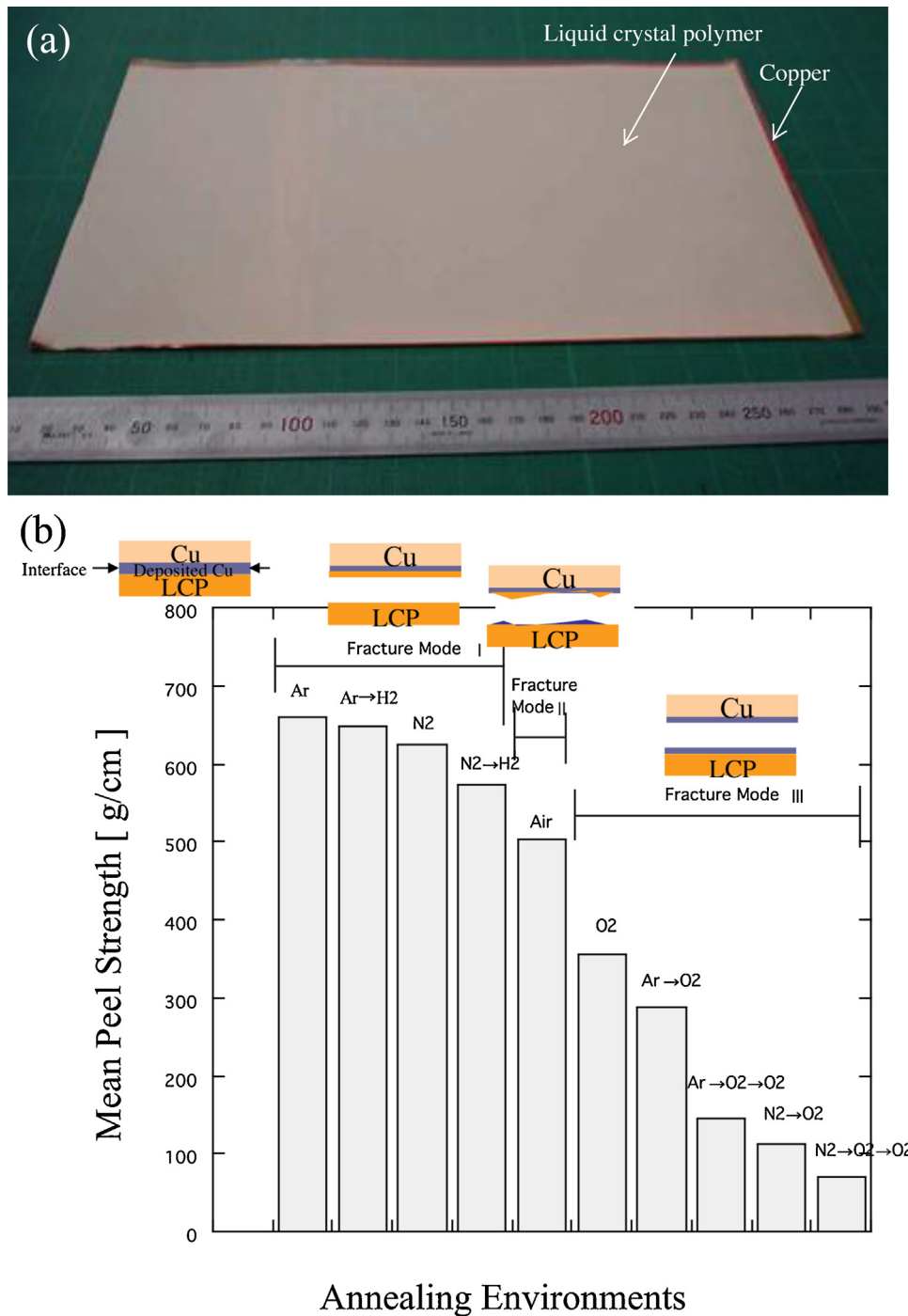
Fig. 2. (a) A sample of LCP laminated on Cu (210 mm × 297 mm) using SAB technology; (b) peel strength of Cu/LCP after annealed in N_2, Ar, air, and O_2 [187].

A high-density brain-machine interface (BMI) device integrating transistors with the electrode arrays on PI substrates has also been presented [281]. High resolution, high speed and low multiplexer crosstalk sampling over large brain areas have been demonstrated in this device. The fabricated 360-channel device covered an area of 10 mm × 9 mm with an electrode size of 300 μm × 300 μm and pitch of 500 μm. Compared with prior work [282], this novel BMI electrode array offered a brain sampling region 5 times larger, but only required one ninth of the wire amount. This technology potentially allows for a large number of channels with high temporal resolution.

The highly flexible PI substrates enable conformal coverage of the device on the tissues. However, the insertion force may cause buckling of the polymer during device implantation. This makes the insertion procedure more difficult than that of using a rigid microelectrode array [283]. A study of the long-term neural implantation of PI showed that its crystalline structure would change, and mechanical properties would degrade due to continuous moisture absorption [56]. The observed increase in Young's modulus and decrease in tensile strength may lead to the increase in plasticity and stiffness of PI. Together with the chemical reactions and the mechanical motions in *in vivo* conditions, the PI packages of the
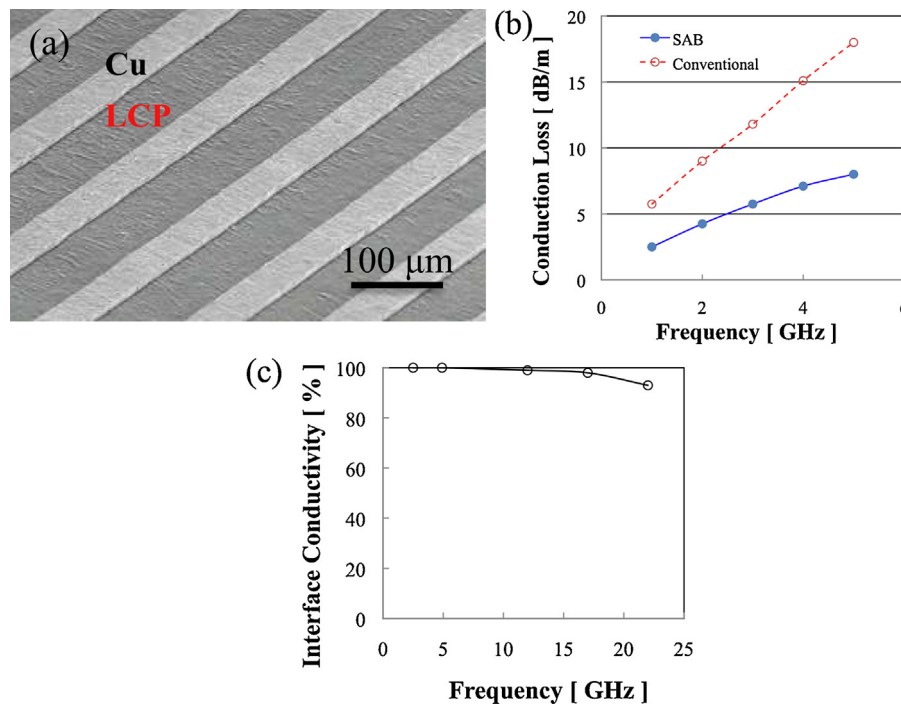
Fig. 3. (a) SEM image of patterned Cu on LCP, sample prepared by SAB; (b) frequency-dependent conduction loss of Cu/LCP interface created by SAB and conventional heat lamination; (c) frequency dependence of the conductivity of Cu/LCP interface created by SAB [196,197].
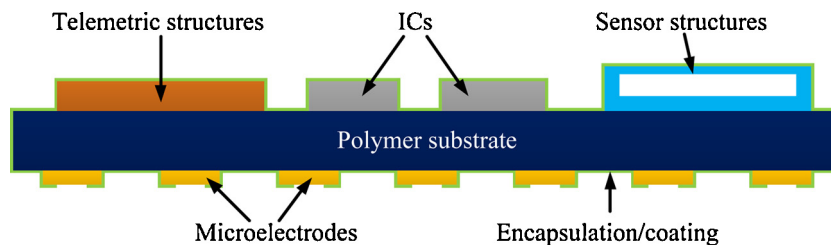
Fig. 4. Conceptual schematic of packaging components in an implantable sensor system.

microelectrode arrays may undergo extra stress, which affects the mechanical compliance of PI with surrounding tissues [284].

4.1.2. PDMS substrates

PDMS has also been employed as a substrate material for microelectrode arrays. Henle et al. [285] have created a trilayer (PDMS-Pt-PDMS) electrode structure by laminating a thin piece of laser-patterned Pt film onto a partially-cured PDMS substrate.

Another PDMS layer was spin-coated on top to form the encapsulant. Dupas-Bruzek et al. [286,287] used a UV laser to chemically activate a PDMS surface and deposited Pt films on top of it using electroless plating. Fabricated electrode arrays were also intended for implantable applications. In contrast to metal films, Hu et al. [288] have developed a way to embed metal nanopowders into the PDMS matrix for microelectrode fabrication. This technique allows for electrodes to be fabricated in high aspect ratio

Table 4
A list of packaging applications of polymer-based implantable sensors.

Applications	Polymer functions	Application challenges	Materials	References
Microelectrode arrays	Substrate Encapsulant/coating	Delamination between polymer and metal, long-term polymer fatigue, elimination of rigid parts, limited electrode locations, required incision process	PI PDMS Parylene LCP	[24,273–282] [285–289] [25,160–162,294–297] [29,190,301,382,383]
Pressure sensors	Substrate Structural components	Implanting space restriction, body movement induced device failure, bio substance stiction induced signal drift, sensitivity	PVDF Parylene PDMS LCP	[82,384] [201,298,299] [27,141,142,304,321–325] [201,272]
Biochemical sensors	SubstrateStructural components	Biocompatibility, signal drift, long-term usage, integration	PDMS	[137,327–329]
Telemetric structures	Substrate Encapsulant/coating	High frequency performance, thermal management	Parylene LCP	[26,203,298,299] [176,272,302]
Implantable systems	Substrate Encapsulant/coating	Hermeticity, biocompatibility, mechanical durability, cost	PEEK Parylene LCP	[337–339,385] [137,157,158,343] [28,191,301,386]

morphologies. In addition, conducting structures made from carbon nanotubes (CNTs) exhibited the properties of large specific capacitance as well as non-Faradaic behavior, which is favored for neuron electrode applications. David-Pur et al. [289] presented a novel flexible neuronal microelectrode device based on multi-wall CNT films embedded in a PDMS layer. The electrodes improved their performance as a result of the combination of several CNT properties: extremely large surface area, good chemical resistivity, and mechanical strength.

As an elastomer, PDMS is permeable to some gases, small molecules, and moisture [290] *in vivo*, which limits its application in packaging of implantable microelectrode arrays. Therefore, sol-gel glass coating [291] and copolymer synthesis [292] have been developed for PDMS to minimize permeability. Also, surface modification of PDMS [293] has been examined to partially address the challenge of protein adsorption [147].

4.1.3. Parylene substrates

Parylene-based ECoG electrode arrays have been developed by Seymour et al. [25] for neural recording and drug delivery applications. The large design space provided a dynamic range of structural stiffness and enabled electrodes to be placed on the front, back or edge of the probe. Results indicated that the use of small edge electrodes improved performance in comparison to conventional planar microelectrodes. Maharbiz's group [294] have reported an optically transparent ECoG electrode array based on a parylene-C and an indium tin oxide conductive layer. Both a 49-channel array (electrode diameter of 500 μm and pitch of 800 μm) and a 16-channel linear array (electrode diameter of 150 μm and pitch of 200 μm) were fabricated. Afterwards, this group enlarged their ECoG electrode array up to 256 channels with the electrode size of 440 μm × 440 μm and pitch of 500 μm [295]. More recently, the same group used these techniques to integrate an antenna with an array of ECoG electrodes on flexible parylene substrate [296]. The system was designed for long-term neural recording within a wireless BMI device. Rodger et al. [297] have demonstrated the use of a high-density electrode array for neural stimulation and recording. The array was on a high-temperature stabilized parylene (parylene-HT) substrate with the electrode diameter of about 10 μm and pitch of less than 50 μm. The authors claimed that it is possible to extend the fabrication process by adding more stacked layers so that an array of 1024 electrodes could be realized within approximately the same area.

Although telemetric components are critical to the signal transmission capabilities of implantable devices, out of all the polymers in Table 2, only parylene and LCP have been widely demonstrated. Tai's group [203,298,299] have used parylene-C to fabricate embedded Au coils through different methods such as surface micromachining and transfer printing. Because of the good high-frequency electrical performance of parylene-C, they realized passive wireless sensing elements with high sensitivity and a quality factor of 30 and higher. The structure was demonstrated by embedding the metal coil in parylene-C layers using thermocompression bonding, as explained in Section 3.1 [203].

Parylene substrates may sustain stable electrical and mechanical contact on tissues. Therefore, an improved signal-to-noise ratio has been demonstrated [300]. However, the poor mechanical strength and robustness of parylene present challenges for device implantation.

4.1.4. LCP substrates

An LCP-based flexible microelectrode array was developed by Lee et al. [190] for retinal prostheses. This microelectrode array was fabricated by means of thermal compression bonding and laser cutting. Accelerated reliability tests prove that such devices have excellent stability in an environment with high humidity and temperature. This might be attributed to LCP's low water uptake ability. Other LCP-Cu based interconnections for retinal and neural prosthetic implants have already been introduced in Section 3.1 [29]. Another group have developed a cortical neural interface microsystem for neural engineering applications [301], containing hybrid RF-inductive and infrared (IR) optical telemetries. This system employed a LCP substrate for the integration of analog, digital, and optoelectronic components. A 16-channel electrode probe was bonded onto the LCP substrate and tested in *in vivo* animal experiments.

A research group has reported LCP-based implants including a multilayered planar coil [176] and an LCP-based eye-surface-conformable telemetric structure [302]. Planar coils used for wireless communication were constructed by the heat lamination of low-temperature LCP and high-temperature LCP with embedded Cu films [176]. The link performance was tested in both *in vitro* and *in vivo* conditions, resulting in a quality factor of 21.15 at 2.54 MHz. The coil could be deformed into a spherical curvature to fit the eyeball surface without affecting its functions or electrical characteristics. Fonseca et al. [272] have reported a flexible micromachined wireless pressure sensor, which was packaged by LCP. The device was highly flexible and could be injected into the body by folding it up into small dimensions. It was tested in canines for over 1 month, and its high reliability was proved by comparing the dynamic pressure waveforms of the implanted and reference sensor. Although it has not been widely demonstrated, LCP is an emerging candidate for implantable components due to its low moisture/gas absorption and permeability.

Polymeric substrates for implantable sensors have considerable advantages over Si ones. Polymers have good mechanical match to soft tissues. They can also easily release the strain induced by external forces. However, many of the electrode arrays are located on the sides of the polymer substrate rather than on the edge. Moreover, their implantation requires an invasive incision to gain access to the tissue.

4.2. Structural component of implantable pressure and biochemical sensors

Structural components, such as pressure sensing membranes and biofluidic channels, can be integrated with polymer substrates in implantable pressure and biochemical sensors. Pressure sensors can be implanted in many locations in the human body. For example, intra-ocular pressure sensors are used for treating patients with glaucoma [303–306]; intra-cranial pressure sensors are employed to assist the therapeutic treatment of intracranial-pressure-related head injuries [307–309]; cardiovascular pressure sensors are implanted in blood vessels or heart chambers to monitor cardiovascular diseases [310–312]; pressure sensors can also be applied in the bladder to diagnose urinary problems [313,314]. While rigid Si-based pressure sensors have been used in these circumstances, flexible polymeric ones are now emerging as substitutes favored by their lower densities, better strain releasing capacity, and lower cost. Biochemical sensors are implanted in the human body for continuous monitoring of certain chemical compositions that cause or aggravate diseases. Examples of implanted biochemical sensors include commercially-available glucose sensors, as well as those for measuring dopamine, glutamate, lactate, ascorbate, reactive oxygen, and nitrogen species in neurological sciences [315].

4.2.1. PVDF structural components

Je et al. [82] introduced a thin film pressure sensor based on PVDF-TrFE copolymer as the structural layer. It was chosen because of its high charge constant, mechanical softness, low modulus, high yield strength, and high resistance to corrosive chemicals [316].

It was fabricated by standard photolithographic patterning of a three-layer structure of metal–(PVDF-TrFE)–metal. The fast recovery time (0.2 s on average), biocompatibility, and compact structure demonstrate the great potential of PVDF-TrFE for use in implants that identify pressure and flow direction. The detected physiological pressure was in the range of 0 to 34 kPa (corresponding to 0.6 to 1 V output voltages). The normal blood pressure (*i.e.*, 13 to 19 kPa) of the human body was included in this range [317]. Furthermore, PVDF-TrFE copolymer has been employed as the gate dielectric layer in a pentacene-based flexible organic field-effect transistor (OFET) on polyethersulfone substrate [83]. Owing to the multi-modal (piezoelectricity and pyroelectricity) sensing properties of PVDF-TrFE copolymer, this device can respond to IR light, pressure, and strain simultaneously. Its high sensitivity towards IR may also allow for applications in biomedical devices that are in direct contact with the human body. Examples include artificial electronic skin, biomedical monitors, and tactile sensors.

In biomedical pressure sensing applications, high sensitivity in the range of 0 to 100 kPa, minimal long-term signal drift, and a robust integration platform is required [318]. *In vivo* piezoelectric pressure sensing is still challenging because of poor sensitivity. To address this issue, PVDF-TrFE, one of the candidate materials, can be applied. However, the device fabrication process, the electrical performance, and the material cost should be optimized.

4.2.2. PDMS structural components

Kim et al. [27] demonstrated a simple fabrication approach for PDMS bladder pressure sensors by utilizing a commercially available thin-film strain gauge embedded in the PDMS diaphragm. Performance validation of the pressure sensors through *in vivo* tests (implanted in a rabbit bladder) was carried out. A measurement resolution of 0.2 kPa was obtained, and the implantable measurement data was consistent with the results of catheter measurement. PDMS has been integrated with graphene to realize a stretchable and biocompatible strain gauge [319]. Its performance was better than conventional metal alloy-based strain gauges [320]. PDMS-cast pressure sensors have also been demonstrated in intraocular applications. Schnakenberg et al. [321,322] and Stangel et al. [304,323,324] presented pressure sensors that were integrated with transponders, which were evaluated in rabbit eyes and showed promising performance. Min et al. [325] have applied reduced graphene oxide (RGO) on both sides of bulk PDMS to fabricate electrodes for pressure-sensitive artificial muscles. As-prepared electrodes exhibited greater electromechanical strain response due to the higher conductivity and flexibility of RGO. Recently, Liu et al. [326] have reported a sensitive planar pressure sensor measuring the resistance changes of Au thin film on PDMS membranes. They demonstrated high performance pressure sensors with a sensitivity of 0.23 per kPa in the measurement range of 0 to 6.67 kPa. The noise-limited resolution was 0.9 Pa and the response time was 200 ms. The strain-induced microcracks contributed to the high sensitivity. So far, the fabricated sensor is the best for biosensing in terms of the reported parameters.

Implantable biochemical sensors, such as glucose sensors, using polymer structural materials have been developed [327–330]. Gough et al. [327] experimentally implanted one of their tissue glucose sensors in a pig for over 1.5 years. The sensor was built up by locating immobilized enzymes in PDMS wells over PDMS-protected electrodes. Macaya et al. [328] have developed a glucose biosensor based on an organic transistor with a conducting channel made of poly(3,4-ethylenedioxythiophene) doped with poly(styrene sulfonate). A PDMS well was again molded and placed on top of a transistor channel that contained analyte solution (phosphate-buffered saline with glucose and glucose–oxidase solution in this case). An all-PDMS-fabricated optical glucose sensor has been designed and fabricated as well [329]. The PDMS material

functioned as the optical waveguide and the transparent substrate in this example, showing high compatibility with the dye/enzyme and analyte system in the sensor. Tsai et al. [137] have presented an integrated implantable multi-analyte biochip system, which includes PDMS-casted micro-channels connected to blood vessels for *in situ* biological signal detection. The micro-channels were fabricated by curing PDMS in a SU-8 photoresist mold, and later transferred to a glass substrate with prefabricated metal detection electrodes.

4.2.3. Parylene structural components

With regard to parylene, Lin et al. [298] reported a new type of intraocular pressure sensor based on their former design [299]. Au electrodes, together with inductor coils, were embedded in thin and flexible parylene layers so that they could attach to the cornea. The sensitivity of this sensor achieved 4 ppm/Pa, which was high enough for intraocular applications. As discussed in Section 3.1, a parylene-parylene thermocompression bonding process for the fabrication of pressure sensors was introduced by Ha's group [201]. This capacitive sensor was designed with an ultra-thin and flexible construction due to the limited space inside the mouse eye for intraocular pressure monitoring. The smallest volume they realized was $300 \times 300 \times 30 \, \mu m^3$ with a high sensitivity of 2.2×10^{-3} fF/Pa.

Apart from biocompatibility, long-term reliability and power consumption issues in implantable pressure and biochemical sensors [331], the remaining challenges include the continuous detection of signals with drift suppression and a suitable data sampling rate. For example, the capacitive sensors consist of fragile membranes that are vulnerable to external mechanical shock, and they require reference pressure when measuring *in vivo* biological signals. Also, piezoresistive sensors are limited by their low sensitivity [318]. Depending on the analyte of biochemical sensors, the structural polymers are normally integrated with different materials, such as metals [332], silver/silver chloride [333], polyaniline nanowires [334], or conducting polypyrrole nanowires [335]. However, conventional integration technologies would either degrade the properties of materials, or increase the production cost of the sensors. Therefore, novel integration technologies are indispensable for realizing the full potential of the passive structures and the active sensing elements for the polymer based sensors.

4.3. Encapsulant and coating of implantable devices

Biocompatible hermetic sealing and coating protects electronic components against the harsh environment of the human body. Requirements for selecting encapsulant/coating materials include [336]: (1) non-toxicity and sterilization; (2) surface biocompatibility to avoid irritating tissues; (3) low permeability to moisture and ionic chemicals; (4) tolerable flexibility and mechanical strength; and (5) long-term reliability. Among these requirements, the moisture absorption and permeation of the encapsulants affect the performance and reliability of the implantable sensors.

4.3.1. PEEK encapsulant

A research group studied the use of PEEK as the packaging material for implantable devices [337–339]. They attempted to solve the adhesion issue between plasma-treated PEEK surfaces and metal films without using adhesives or other agents. It was found that maximum adhesion strength can be obtained by tuning plasma process parameters with the aim of increasing the surface energy of PEEK.

4.3.2. Parylene coating

As one of the examples described in Section 4.2 [137], the implantable microfluidic biochemical sensing system should be packaged inside of a shell made of biocompatible materials. Thus,

5 μm thick parylene-C was coated at the exterior side of the device to ensure no biorejection would occur. In another study, DeHennis et al. [340] used 1 μm parylene-C coating outside a fully integrated pressure sensing and wireless communication system to maintain a biocompatible interface and electrical isolation. Parylene was selected mainly due to its reduced water absorption compared to silicone [341]. It was used as the secondary barrier layer to protect the components from the harsh environment. Furthermore, in applications of the ECoG electrode arrays, parylene-C was used not only as the substrate material, but also as the encapsulant layer. The encapsulation was demonstrated by Winkin and Mokwa [342], who deposited parylene-C from its gas phase to seal the metal structures. Yu et al. [343] have coated nickel microprobe electrodes with parylene thin film to improve the biocompatibility of the implantable device. In this system, the implanted probe array was connected with extra-body bond pads by connecting a 42 mm-long parylene cable with Au connection wires on it. The neural activities in a rat's hippocampus were recorded with high quality using this device. Also, the wing beat stimulations of honeybees were achieved by injecting pulse signals.

4.3.3. LCP encapsulant

An implantable neuroprosthetic device has been developed using an LCP encapsulant [191]. The cover lid was fabricated by thermoforming LCP into the desired geometry for the caged ICs and telemetry coils. The LCP lid and substrate were fusion-bonded together to realize the hermetic package, the performance of which was evaluated using *in vitro* soak tests. The results showed that the LCP package obtained a higher long-term reliability with regard to hermeticity when compared with PI and parylene packages. Very recently, the same research group used a similar technology and developed a way for producing LCP-encapsulated monolithic RFIC devices for biomedical wireless communication [28]. This new LCP-packaged device has been successfully implanted and tested in a live rat.

Biocompatible encapsulants and coatings are intended to reduce unwanted biological responses, such as inflammatory responses, and foreign body reactions [344–346]. Although there are other encapsulant materials, such as poly(hydroxyethyl methacrylate) [347,348], poly(vinyl alcohol) [349], poly(ethylene glycol) [350], and PU [351,352], they are structurally unsuitable for implantable sensors. In another aspect, while the weight and volume of the electronic components are decreasing, those of the encapsulants are not significantly changed. Further, coupling capacitors are needed to prevent tissue damage and component corrosion. The capacitors can balance the charge and minimize the leakage current, but may increase the volume of the device [353,354]. Consequently, advanced integration and packaging technologies for biocompatible encapsulant and coating materials are needed in order to produce light-weight and small-volume implantable sensors.

5. Conclusions and perspectives

In the packaging of implantable sensors [355], light-weight and low-cost polymer-based materials have been studied and utilized because of their superior biocompatibility, chemical resistivity, mechanical flexibility, and optical transparency to metals and ceramics. Reliable emerging sensors may include components such as microelectrode arrays, telemetric structures, and sensing structures, which need fine-pitch, low-loss, and high-performance conductive paths on the polymer films. Thus, advanced packaging materials and integration processes are required for their fabrication. This article reviews the properties of specific polymers and their integration technologies and provides an overview of emerging implantable sensors. It is challenging for many polymers to

meet the requirements of the implantable sensors due to their high moisture absorption rate, high electrical loss, and low mechanical stability. LCP has been found to be one of the desirable materials for packaging of next-generation implantable sensors due to its superior properties as well as its potential for mass production compared with other polymers.

For the integration of polymer–polymer/metal in implantable sensors, SAB technologies are highly promising because they offer nanoscaled bonded interfaces at low temperature. The bonded interfaces are highly reliable and biocompatible with low/minimal degradation of the bonded materials. The SAB interface of polymer/metal shows better performance over other methods because it does not require high temperature, high pressure, or a thick intermediate layer. This article compares the properties of different polymeric materials and categorizes various polymer–polymer/metal integration technologies for implantable packages. It is suggested that proper materials and technologies should be selected according to the pros and cons of each material-process combination.

In the future, polymer-related integration technologies need to be further developed for packaging of high performance implantable sensors. Firstly, the technical challenges, such as the long processing time in SAB, need to be addressed along with demonstrations of packaging of implantable sensors. Secondly, there is a demand to fabricate organic ICs (rather than conventional Si ICs) on flexible substrates using the advanced polymer integration technologies. However, the surface roughness of thin films greatly affects the performance of the devices [356–358]. To address this issue, the SAB technologies together with UV irradiation [359], polymer planarization with activation [358], and electropolishing [360] have been applied. Thirdly, small and high-density patterns need to be created on flexible substrates for the parallel recording of bio-signals. Fourthly, the integration opportunities of various thin-layers in the SAB allow for the creation of light-weight and small-volume coupling capacitors, which minimizes the leakage current.

While polymers provide opportunities in implantable devices, there are further issues yet to be completely understood. The crucial challenge may be the requirement for an interdisciplinary knowledge of polymer-based sensor packaging. This review article guides and bridges emerging research in polymer-related materials, electronics, and biomedical technologies to develop integrated systems for reliable, high-performance implantable sensors at low cost.

References

[1] D.-H. Kim, J. Viventi, J.J. Amsden, J. Xiao, L. Vigeland, Y.-S. Kim, J.A. Blanco, B. Panilaitis, E.S. Frechette, D. Contreras, Dissolvable films of silk fibroin for ultrathin conformal bio-integrated electronics, Nat. Mater. 9 (2010) 511–517.

[2] G. Jiang, D.D. Zhou, Technology Advances and Challenges in Hermetic Packaging for Implantable Medical Devices, Springer, New York, NY, USA, 2010.

[3] D.F. Williams, Biocompatibility of Clinical Implant Materials, CRC Press, Boca Raton, FL, USA, 1981.

[4] R. Thomas, Moisture, myths, and microcircuits, IEEE Trans. Parts, Hybrids, Packag. 12 (1976) 167–171.

[5] A. DerMarderosian, The electrochemical migration of metals, in: International Microelectronics Symposium, Montgomery, AL, USA, 1978, pp. 134–141.

[6] M. Forde, P. Ridgely, Implantable Cardiac Pacemakers, CRC Press, Boca Raton, FL, USA, 2006.

[7] M.J. Deen, R. Murji, A. Fakhr, N. Jafferali, W.L. Ngan, Low-power CMOS integrated circuits for radio frequency applications, IEE Proc.—Circ. Dev. Syst. 152 (2005) 509–522.

[8] S.F. Hulbert, J.C. Bokros, L.L. Hench, J. Wilson, G. Heimke, Ceramics in clinical applications, past, present and future, in: High Tech Ceramics: Proceedings of the World Congress on High Tech Ceramics, the Sixth International Meeting on Modern Ceramics Technologies (6th CIMTEC), Milan, Italy, 1986, pp. 189–213.

[9] L.L. Hench, Clinical Performance of Skeletal Prostheses, Springer, Berlin, Germany, 1996.

[10] C. Piconi, G. Maccauro, Zirconia as a ceramic biomaterial, Biomaterials 20 (1999) 1–25.

[11] E.A. Griffin, D.R. Mumm, D.B. Marshall, Rapid prototyping of functional ceramic composites, Am. Ceram. Soc. Bull. 75 (1996) 65–70.

[12] G. Jiang, Development of Ceramic-to-Metal Package for BION Microstimulator, Biomedical Engineering Department, University of Southern California, Los Angeles, CA, USA, 2005.

[13] I. Hochmair, P. Nopp, C. Jolly, M. Schmidt, H. Schößer, C. Garnham, I. Anderson, MED-EL cochlear implants: state of the art and a glimpse into the future, Trends Amplif. 10 (2006) 201–219.

[14] J.D. Weiland, W. Liu, M.S. Humayun, Retinal prosthesis, Annu. Rev. Biomed. Eng. 7 (2005) 361–401.

[15] A.K. Ahuja, J.D. Dorn, A. Caspi, M.J. McMahon, G. Dagnelie, P. Stanga, M.S. Humayun, R.J. Greenberg, Blind subjects implanted with the Argus II retinal prosthesis are able to improve performance in a spatial-motor task, Br. J. Ophthalmol. 95 (2011) 539–543.

[16] E. Zrenner, K.U. Bartz-Schmidt, H. Benav, D. Besch, A. Bruckmann, V.-P. Gabel, F. Gekeler, U. Greppmaier, A. Harscher, S. Kibbel, Subretinal electronic chips allow blind patients to read letters and combine them to words, Proc. R. Soc. London, Ser. B 278 (2011) 1489–1497.

[17] N.R. Srivastava, P.R. Troyk, G. Dagnelie, Detection, eye-hand coordination and virtual mobility performance in simulated vision for a cortical visual prosthesis device, J. Neural Eng. 6 (2009) 035008.

[18] L.R. Hochberg, M.D. Serruya, G.M. Friehs, J.A. Mukand, M. Saleh, A.H. Caplan, A. Branner, D. Chen, R.D. Penn, J.P. Donoghue, Neuronal ensemble control of prosthetic devices by a human with tetraplegia, Nature 442 (2006) 164–171.

[19] R. Ljung, P. Petrini, A.-K. Lindgren, E. Berntorp, Implantable central venous catheter facilitates prophylactic treatment in children with haemophilia, Acta Paediatr. 81 (1992) 918–920.

[20] D.F. Lovely, M.B. Olive, R.N. Scott, Epoxy moulding system for the encapsulation of microelectronic devices suitable for implantation, Med. Biol. Eng. Comput. 24 (1986) 206–208.

[21] A. Krebs, T. Knoll, D. Nußbaum, T. Velten, Polymer-based fabrication techniques for enclosed microchannels in biomedical applications, Microsyst. Technol. 18 (2012) 1871–1877.

[22] P.E.K. Donaldson, The Cooper cable: an implantable multiconductor cable for neurological prostheses, Med. Biol. Eng. Comput. 21 (1983) 371–374.

[23] V. Thomas, M. Jayabalan, A new generation of high flex life polyurethane urea for polymer heart valve-studies on *in vivo* biocompatibility and biodurability, J. Biomed. Mater. Res., A 89 (2009) 192–205.

[24] E. Patrick, M. Ordonez, N. Alba, J.C. Sanchez, T. Nishida, Design and fabrication of a flexible substrate microelectrode array for brain machine interfaces, in: EMBS'06 28th Annual International Conference of the IEEE Engineering in Medicine and Biology Society, New York, NY, USA, 2006, pp. 2966–2969.

[25] J.P. Seymour, N.B. Langhals, D.J. Anderson, D.R. Kipke, Novel multi-sided, microelectrode arrays for implantable neural applications, Biomed. Microdevices 13 (2011) 441–451.

[26] J.P. Seymour, Y.M. Elkasabi, H.-Y. Chen, J. Lahann, D.R. Kipke, The insulation performance of reactive parylene films in implantable electronic devices, Biomaterials 30 (2009) 6158–6167.

[27] J. Kim, H. Lee, S. Cha, B. Choi, Fabrication and evaluation of implantable pressure sensor using strain gauge, in: Biomedical Engineering International Conference (BMEiCON), Ubon Ratchathani, Thailand, 2012, pp. 1–4.

[28] G.-T. Hwang, D. Im, S.E. Lee, J. Lee, M. Koo, S.Y. Park, S. Kim, K. Yang, S.J. Kim, K. Lee, *In vivo* silicon-based flexible radio frequency integrated circuits monolithically encapsulated with bio-compatible liquid crystal polymers, ACS Nano 7 (2013) 4545–4553.

[29] V. Sundaram, V. Sukumaran, M.E. Cato, F. Liu, R. Tummala, P.J. Nasiatka, J.D. Weiland, A.R. Tanguay, High density electrical interconnections in liquid crystal polymer (LCP) substrates for retinal and neural prosthesis applications, in: 2011 IEEE 61st Electronic Components and Technology Conference (ECTC), Lake Buena Vista, FL, USA, 2011, pp. 1308–1313.

[30] D. Ha, B.G. Kim, T.-Y. Lin, Y. Ouyang, P.P. Irazoqui, W.J. Chappell, 3D packaging technique on liquid crystal polymer (LCP) for miniature wireless biomedical sensor, in: 2010 IEEE MTT-S International Microwave Symposium Digest (MTT), Anaheim, CA, USA, 2010, pp. 612–615.

[31] H. Hassler, T. Boretius, T. Stieglitz, Polymers for neural implants, J. Polym. Sci., B: Polym. Phys. 49 (2011) 18–33.

[32] M.M.R. Howlader, P.R. Selvaganapathy, M.J. Deen, T. Suga, Nanobonding technology toward electronic, fluidic, and photonic systems integration, IEEE J. Sel. Top. Quantum Electron. 17 (2011) 689–703.

[33] B. Ghane-Motlagh, M. Sawan, A review of microelectrode array technologies: design and implementation challenges, in: Second International Conference on Advances in Biomedical Engineering (ICABME), Tripoli, Lebanon, 2013, pp. 38–41.

[34] B. Ghane-Motlagh, M. Sawan, Design and implementation challenges of microelectrode arrays: a review, Mater. Sci. Appl. 4 (2013) 483–495.

[35] C. Pang, C. Lee, K.-Y. Suh, Recent advances in flexible sensors for wearable and implantable devices, J. Appl. Polym. Sci. 130 (2013) 1429–1441.

[36] S. Venkatraman, F. Boey, L.L. Lao, Implanted cardiovascular polymers: natural, synthetic and bio-inspired, Prog. Polym. Sci. 33 (2008) 853–874.

[37] S. Ramakrishna, J. Mayer, E. Wintermantel, K.W. Leong, Biomedical applications of polymer-composite materials: a review, Compos. Sci. Technol. 61 (2001) 1189–1224.

[38] S.-C. Luo, Conducting polymers as biointerfaces and biomaterials: a perspective for a special issue of polymer reviews, Polym. Rev. 53 (2013) 303–310.

[39] L. Xia, Z. Wei, M. Wan, Conducting polymer nanostructures and their application in biosensors, J. Colloid Interface Sci. 341 (2010) 1–11.

[40] S.P. Lyu, D. Untereker, Degradability of polymers for implantable biomedical devices, Int. J. Mol. Sci. 10 (2009) 4033–4065.

[41] T. Stieglitz, M. Schuettler, J.-U. Meyer, Micromachined, polyimide-based devices for flexible neural interfaces, Biomed. Microdevices 2 (2000) 283–294.

[42] J.-S. Jiang, B.-S. Chiou, The effect of polyimide passivation on the electromigration of Cu multilayer interconnections, J. Mater. Sci.: Mater. Electron. 12 (2001) 655–659.

[43] A.B. Frazier, Recent applications of polyimide to micromachining technology, IEEE Trans. Ind. Electron. 42 (1995) 442–448.

[44] B. Stark, MEMS reliability assurance guidelines for space applications, Jet Propulsion Laboratory, JPL Publication, Pasadena, CA, USA, 1999.

[45] J. Laconte, V. Wilmart, D. Flandre, J.P. Raskin, High-sensitivity capacitive humidity sensor using 3-layer patterned polyimide sensing film, in: Proceedings IEEE Sensors Conference, Toronto, Canada, 2003, pp. 372–377.

[46] M. Sato, T. Yamamoto, M. Takeuchi, K. Yamanouchi, Humidity sensitivity of lamb waves on composite polyimide/ZnO/Si$_3$N$_4$ structure, Jpn. J. Appl. Phys. 32 (1993) 2380–2383.

[47] L.K. Lagorce, M.G. Allen, Magnetic and mechanical properties of micromachined strontium ferrite/polyimide composites, J. Microelectromech. Syst. 6 (1997) 307–312.

[48] J.W. Judy, N. Myung, Magnetic materials for MEMS, in: Materials Research Society (MRS) Workshop on MEMS Materials, San Francisco, CA, USA, 2002, pp. 23–26.

[49] J.D. Sternhagen, C.E. Wold, W.A. Kempf, M. Karlgaard, K.D. Mitzner, R.D. Mileham, D.W. Galipeau, A novel integrated acoustic gas and temperature sensor, IEEE Sens. J. 2 (2002) 301–306.

[50] F. Jiang, Y.-C. Tai, K. Walsh, T. Tsao, G.-B. Lee, C.-M. Ho, A flexible MEMS technology and its first application to shear stress sensor skin, in: MEMS'97 10th Annual International Workshop on Micro Electro Mechanical Systems, Nagoya, Japan, 1997, pp. 465–470.

[51] W.C. Wilson, G.M. Atkinson, Review of polyimides used in the manufacturing of micro systems, in: Technical Report, NASA/TM-2007-214870, L-19339, NASA Langley Research Center, Hampton, VA, USA, 2007.

[52] R.R. Richardson Jr., J.A. Miller, W.M. Reichert, Polyimides as biomaterials: preliminary biocompatibility testing, Biomaterials 14 (1993) 627–635.

[53] W. Li, J.-L. Zhang, H.-M. Li, T. Ding, L. Wang, Preparation of ultrafiltration membranes with aromatic polyimide, in: Fifth International Membrane Science & Technology Conference, Sydney, Australia, 2003, pp. 1–6.

[54] Analog Devices, iCoupler® Products with isoPower™ Technology: Signal and Power Transfer across Isolation Barrier Using Microtransformers, Analog Devices, 2006, http://communications.analog.com/static/imported-files/tech_docs/isoPower.pdf.

[55] T. Akin, K. Najafi, R.H. Smoke, R.M. Bradley, A micromachined silicon sieve electrode for nerve regeneration applications, IEEE Trans. Biomed. Eng. 41 (1994) 305–313.

[56] B. Rubehn, T. Stieglitz, *In vitro* evaluation of the long-term stability of polyimide as a material for neural implants, Biomaterials 31 (2010) 3449–3458.

[57] N. Lago, D. Ceballos, F.J. Rodríguez, T. Stieglitz, X. Navarro, Long term assessment of axonal regeneration through polyimide regenerative electrodes to interface the peripheral nerve, Biomaterials 26 (2005) 2021–2031.

[58] X. Navarro, T.B. Krueger, N. Lago, S. Micera, T. Stieglitz, P. Dario, A critical review of interfaces with the peripheral nervous system for the control of neuroprostheses and hybrid bionic systems, J. Peripher. Nerv. Syst. 10 (2005) 229–258.

[59] T. Boretius, J. Badia, A. Pascual-Font, M. Schuettler, X. Navarro, K. Yoshida, T. Stieglitz, A transverse intrafascicular multichannel electrode (TIME) to interface with the peripheral nerve, Biosens. Bioelectron. 26 (2010) 62–69.

[60] M. HajjHassan, V. Chodavarapu, S. Musallam, NeuroMEMS: neural probe microtechnologies, Sensors 8 (2008) 6704–6726.

[61] UBE, UBE U-Varnish Material Data Sheet, 2009, http://www.ube.com/content.php?pageid=83.

[62] H.S. Nalwa, Ferroelectric Polymers: Chemistry, Physics, and Applications, CRC Press, New York, NY, USA, 1995.

[63] H. Kawai, The piezoelectricity of poly(vinylidene fluoride), Jpn. J. Appl. Phys. 8 (1969) 975–976.

[64] K. Omote, H. Ohigashi, K. Koga, Temperature dependence of elastic, dielectric, and piezoelectric properties of "single crystalline" films of vinylidene fluoride trifluoroethylene copolymer, J. Appl. Phys. 81 (1997) 2760–2769.

[65] Y. Jiang, H. Hamada, S. Shiono, K. Kanda, T. Fujita, K. Higuchi, K. Maenaka, A PVDF-based flexible cardiorespiratory sensor with independently optimized sensitivity to heartbeat and respiration, Procedia Eng. 5 (2010) 1466–1469.

[66] J. Cai, X. Fu, H. Liu, Design of PVDF stress sensor and its application in the stress test of foam plastic, in: 2012 International Conference on Measurement, Information and Control (MIC), Harbin, China, 2012, pp. 821–824.

[67] M. Kurata, X. Li, K. Fujita, L. He, M. Yamaguchi, PVDF piezo film as dynamic strain sensor for local damage detection of steel frame buildings, in: SPIE Sensors and Smart Structures Technologies for Civil, Mechanical, and Aerospace Systems Conference, San Diego, CA, USA, 2013, p. 86920F.

[68] Z. Sun, L. Hao, S. Li, J. Shen, A PVDF micro-force sensor based on inverse-model algorithm and its applications, in: 2011 IEEE International Conference on Information and Automation (ICIA), Shenzhen, China, 2011, pp. 801–806.

[69] C. Sun, J. Shi, D.J. Bayerl, X. Wang, PVDF microbelts for harvesting energy from respiration, Energy Environ. Sci. 4 (2011) 4508–4512.

[70] Y.G. Jiang, S. Shiono, H. Hamada, T. Fujita, K. Higuchi, K. Maenaka, Low-frequency energy harvesting using a laminated PVDF cantilever with a magnetic mass, in: PowerMEMS 2010: the 10th International Workshop on Micro and Nanotechnology for Power Generation and Energy Conversion Applications, Leuven, Belgium, 2010, pp. 375–378.

[71] S. Dey, M. Purahmad, S. Sinha-Ray, A.L. Yarin, M. Dutta, Investigation of PVDF-TrFE nanofibers for energy harvesting, in: 2012 IEEE Conference on Nanotechnology Materials and Devices Conference (NMDC), Waikiki Beach, HI, USA, 2012, pp. 21–24.

[72] S.-D. Hu, K.-C. Chuang, H.-S. Tzou, PVDF energy harvester on flexible rings, in: 2010 Symposium on Piezoelectricity, Acoustic Waves and Device Applications (SPAWDA), Xiamen, China, 2010, pp. 100–105.

[73] E. Urban, M.W. King, R. Guidoin, G. Laroche, Y. Marois, L. Martin, A. Cardou, Y. Douville, Why make monofilament sutures out of polyvinylidene fluoride? ASAIO J. 40 (1994) 145–156.

[74] Arkema Inc., KYNAR® & KYNAR FLEX® PVDF, Performance Characteristics & Data, 2011, http://www.arkema-inc.com/kynar/literature/pdf/743.pdf.

[75] G. Laroche, Y. Marois, R. Guidoin, M.W. King, L. Martin, T. How, Y. Douville, Polyvinylidene fluoride (PVDF) as a biomaterial: from polymeric raw material to monofilament vascular suture, J. Biomed. Mater. Res. 29 (1995) 1525–1536.

[76] U. Klinge, B. Klosterhalfen, A.P. Öttinger, K. Junge, V. Schumpelick, PVDF as a new polymer for the construction of surgical meshes, Biomaterials 23 (2002) 3487–3493.

[77] U. Klinge, M. Anurov, S. Titkova, P.R. Mertens, M. Jansen, Surgical mesh as a scaffold for tissue regeneration in the esophagus, Eur. Surg. Res. 36 (2004) 104–111.

[78] K. Junge, R. Rosch, U. Klinge, C. Krones, B. Klosterhalfen, P.R. Mertens, P. Lynen, D. Kunz, A. Preiß, H. Peltroche-Llacsahuanga, Gentamicin supplementation of polyvinylidenfluoride mesh materials for infection prophylaxis, Biomaterials 26 (2005) 787–793.

[79] G. Laroche, Y. Marois, E. Schwarz, R. Guidoin, M.W. King, E. Pâris, Y. Douville, Polyvinylidene fluoride monofilament sutures: can they be used safely for long-term anastomoses in the thoracic aorta? Artif. Organs 19 (1995) 1190–1199.

[80] M. Parirokh, S. Asgary, M.J. Eghbal, S. Stowe, S. Kakoei, A scanning electron microscope study of plaque accumulation on silk and PVDF suture materials in oral mucosa, Int. Endod. J. 37 (2004) 776–781.

[81] J.F. Mano, J.L. Lopes, R.A. Silva, W. Brostow, Creep of PVDF monofilament sutures: service performance prediction from short-term tests, Polymer 44 (2003) 4293–4300.

[82] S.-S. Je, T. Sharma, Y. Lee, B. Gill, J.X. Zhang, A thin-film piezoelectric PVDF-TrFE based implantable pressure sensor using lithographic patterning, in: 2011 IEEE 24th International Conference on Micro Electro Mechanical Systems (MEMS), Cancun, Mexico, 2011, pp. 644–647.

[83] T.Q. Trung, N.T. Tien, Y.G. Seol, N.-E. Lee, Transparent and flexible organic field-effect transistor for multi-modal sensing, Org. Electron. 13 (2012) 533–540.

[84] J. Scheirs, S. Burks, A. Locaspi, Development in fluoropolymer coatings, Trends Polym. Sci. 3 (1995) 74–82.

[85] O.B. Wilson, Introduction to Theory and Design of Sonar Transducers, Peninsula, Los Altos CA, USA, 1988.

[86] J.E. Mark, Polymer Data Handbook, Oxford University Press, New York, NY, USA, 2009.

[87] D.P. Jones, D.C. Leach, D.R. Moore, Mechanical properties of poly(ether-ether-ketone) for engineering applications, Polymer 26 (1985) 1385–1393.

[88] R.A. Chivers, D.R. Moore, The effect of molecular weight and crystallinity on the mechanical properties of injection moulded poly(aryl-ether-ether-ketone) resin, Polymer 35 (1994) 110–116.

[89] P.J. Rae, E.N. Brown, E.B. Orler, The mechanical properties of poly(ether-ether-ketone) (PEEK) with emphasis on the large compressive strain response, Polymer 48 (2007) 598–615.

[90] M. Brillhart, B.L. Gregory, J. Botsis, Fatigue fracture behaviour of PEEK: 1. Effects of load level, Polymer 32 (1991) 1605–1611.

[91] M. Brillhart, J. Botsis, Fatigue fracture behaviour of PEEK: 2. Effects of thickness and temperature, Polymer 33 (1992) 5225–5232.

[92] C.M. Cady, W.R. Blumenthal, G.T. Gray III, D.J. Idar, Determining the constitutive response of polymeric materials as a function of temperature and strain rate, J. Phys. IV France 110 (2003) 27–32.

[93] S. Hamdan, G.M. Swallowe, The strain-rate and temperature dependence of the mechanical properties of polyetherketone and polyetheretherketone, J. Mater. Sci. 31 (1996) 1415–1423.

[94] R.T.S.M. Lakshmi, V. Choudhary, I.K. Varma, Sulphonated poly(ether ether ketone): synthesis and characterisation, J. Mater. Sci. 40 (2005) 629–636.

[95] K.C. Cole, I.G. Casella, Fourier transform infrared spectroscopic study of thermal degradation in films of poly(etheretherketone), Thermochim. Acta 211 (1992) 209–228.

[96] M. Buggy, A. Carew, The effect of thermal ageing on carbon fibre-reinforced polyetheretherketone (PEEK), J. Mater. Sci. 29 (1994) 2255–2259.

[97] J.N. Hay, D.J. Kemmish, Thermal decomposition of poly(aryl ether ketones), Polymer 28 (1987) 2047–2051.

[98] M.R. Meyer, R.J. Friedman, H. Del Schutte, R.A. Latour, Long-term durability of the interface in FRP composites after exposure to simulated physiologic saline environments, J. Biomed. Mater. Res. 28 (1994) 1221–1231.

[99] E. Boinard, R.A. Pethrick, C.J. MacFarlane, The influence of thermal history on the dynamic mechanical and dielectric studies of polyetheretherketone exposed to water and brine, Polymer 41 (2000) 1063–1076.

[100] E.J. Stober, J.C. Seferis, J.D. Keenan, Characterization and exposure of polyetheretherketone (PEEK) to fluid environments, Polymer 25 (1984) 1845–1852.

[101] S.M. Kurtz, J.N. Devine, PEEK biomaterials in trauma, orthopedic, and spinal implants, Biomaterials 28 (2007) 4845–4869.

[102] D.R. McKenzie, K. Newton-McGee, P. Ruch, M.M. Bilek, B.K. Gan, Modification of polymers by plasma-based ion implantation for biomedical applications, Surf. Coat. Technol. 186 (2004) 239–244.

[103] S. Akhavan, M.M. Matthiesen, L. Schulte, T. Penoyar, M.J. Kraay, C.M. Rimnac, V.M. Goldberg, Clinical and histologic results related to a low-modulus composite total hip replacement stem, J. Bone Jt. Surg. 88 (2006) 1308–1314.

[104] J.W. Brantigan, A. Neidre, J.S. Toohey, The Lumbar I/F Cage for posterior lumbar interbody fusion with the variable screw placement system: 10-year results of a food and drug administration clinical trial, Spine J. 4 (2004) 681–688.

[105] J.M. Toth, M. Wang, B.T. Estes, J.L. Scifert, H.B. Seim III, A.S. Turner, Polyetheretherketone as a biomaterial for spinal applications, Biomaterials 27 (2006) 324–334.

[106] T.J. Joyce, C. Rieker, A. Unsworth, Comparative *in vitro* wear testing of PEEK and UHMWPE capped metacarpophalangeal prostheses, Bio-Med. Mater. Eng. 16 (2006) 1–10.

[107] A. Wang, R. Lin, C. Stark, J.H. Dumbleton, Suitability and limitations of carbon fiber reinforced PEEK composites as bearing surfaces for total joint replacements, Wear 225 (1999) 724–727.

[108] C.-H. Rivard, S. Rhalmi, C. Coillard, In vivo biocompatibility testing of peek polymer for a spinal implant system: a study in rabbits, J. Biomed. Mater. Res. 62 (2002) 488–498.

[109] K. Liao, Performance characterization and modeling of a composite hip prosthesis, Exp. Tech. 18 (1994) 33–38.

[110] G.R. Maharaj, R.D. Jamison, Intraoperative impact: characterization and laboratory simulation on composite hip prostheses, ASTM Spec. Tech. Publ. 1178 (1993), 98 - 98.

[111] D.J. Kelsey, G.S. Springer, S.B. Goodman, Composite implant for bone replacement, J. Compos. Mater. 31 (1997) 1593–1632.

[112] A.A. Corvelli, P.J. Biermann, J.C. Roberts, Design, analysis, and fabrication of a composite segmental bone replacement implant, J. Adv. Mater. 28 (1997) 2–8.

[113] S.A. Brown, R.S. Hastings, J.J. Mason, A. Moet, Characterization of short-fibre reinforced thermoplastics for fracture fixation devices, Biomaterials 11 (1990) 541–547.

[114] I. Yakimets, D. MacKerron, P. Giesen, K.J. Kilmartin, E. Meinders, W.A. MacDonald, Polymer substrates for flexible electronics: achievements and challenges, Adv. Mater. Res. 93 (2010) 5–8.

[115] D. Briem, S. Strametz, K. Schröoder, N.M. Meenen, W. Lehmann, W. Linhart, A. Ohl, J.M. Rueger, Response of primary fibroblasts and osteoblasts to plasma treated polyetheretherketone (PEEK) surfaces, J. Mater. Sci.: Mater. Med. 16 (2005) 671–677.

[116] A. Ito, K. Maekawa, S. Tsutsumi, F. Ikazaki, T. Tateishi, Solubility product of OH-carbonated hydroxyapatite, J. Biomed. Mater. Res. 36 (1997) 522–528.

[117] J.G. Drobny, Handbook of Thermoplastic Elastomers, Elsevier, Amsterdam, The Netherlands, 2007.

[118] D. Armani, C. Liu, N. Aluru, Re-configurable fluid circuits by PDMS elastomer micromachining, in: MEMS'99. Twelfth IEEE International Conference on Micro Electro Mechanical Systems, Orlando, FL, USA, 1999, pp. 222–227.

[119] S.J. Clarson, J.A. Semlyen, Siloxane Polymers, PTR Prentice Hall, New York, USA, 1993.

[120] M. Bender, U. Plachetka, J. Ran, A. Fuchs, B. Vratzov, H. Kurz, T. Glinsner, F. Lindner, High resolution lithography with PDMS molds, J. Vac. Sci. Technol., B 22 (2004) 3229–3232.

[121] J.C. Lötters, W. Olthuis, P.H. Veltink, P. Bergveld, The mechanical properties of the rubber elastic polymer polydimethylsiloxane for sensor applications, J. Micromech. Microeng. 7 (1997) 145–147.

[122] T.-K. Shih, C.-F. Chen, J.-R. Ho, F.-T. Chuang, Fabrication of PDMS (polydimethylsiloxane) microlens and diffuser using replica molding, Microelectron. Eng. 83 (2006) 2499–2503.

[123] D. Szmigiel, K. Domański, P. Prokaryn, P. Grabiec, Deep etching of biocompatible silicone rubber, Microelectron. Eng. 83 (2006) 1178–1181.

[124] J. Garra, T. Long, J. Currie, T. Schneider, R. White, M. Paranjape, Dry etching of polydimethylsiloxane for microfluidic systems, J. Vac. Sci. Technol., A 20 (2002) 975–982.

[125] M. Schuettler, C. Henle, J. Ordonez, G.J. Suaning, N.H. Lovell, T. Stieglitz, Patterning of silicone rubber for micro-electrode array fabrication, in: CNE'07 Third International IEEE/EMBS Conference on Neural Engineering, Kohala Coast, HI, USA, 2007, pp. 53–56.

[126] J.S. Kuo, D.T. Chiu, Disposable microfluidic substrates: transitioning from the research laboratory into the clinic, Lab Chip 11 (2011) 2656–2665.

[127] G.S. Brindley, The first 500 patients with sacral anterior root stimulator implants: general description, Spinal Cord 32 (1994) 795–805.

[128] R. Yoda, Elastomers for biomedical applications, J. Biomater. Sci., Polym. Ed. 9 (1998) 561–626.

[129] T.J. Joyce, A. Unsworth, The wear of artificial finger joints using different lubricants in a new finger wear simulator, Wear 250 (2001) 199–205.

[130] T. Motomura, T. Maeda, S. Kawahito, T. Matsui, S. Ichikawa, H. Ishitoya, M. Kawamura, T. Shinohara, K. Sato, Y. Kawaguchi, Development of silicone rubber hollow fiber membrane oxygenator for ECMO, Artif. Organs 27 (2003) 1050–1053.

[131] R.M. Goldblum, A.A. O'Donell, D. Pyron, R.P. Pelley, J.P. Heggers, Antibodies to silicone elastomers and reactions to ventriculoperitoneal shunts, Lancet 340 (1992) 510–513.

[132] A. Backovic, D. Wolfram, B. Del-Frari, H. Piza, L.A. Huber, G. Wick, Simultaneous analysis of multiple serum proteins adhering to the surface of medical grade polydimethylsiloxane elastomers, J. Immunol. Methods 328 (2007) 118–127.

[133] M.-W. Moon, S.H. Lee, J.-Y. Sun, K.H. Oh, A. Vaziri, J.W. Hutchinson, Wrinkled hard skins on polymers created by focused ion beam, Proc. Nat. Acad. Sci. U.S.A. 104 (2007) 1130–1133.

[134] L.J. Millet, M.E. Stewart, J.V. Sweedler, R.G. Nuzzo, M.U. Gillette, Microfluidic devices for culturing primary mammalian neurons at low densities, Lab Chip 7 (2007) 987–994.

[135] P. Rezai, P.R. Selvaganapathy, G.R. Wohl, Plasma enhanced bonding of polydimethylsiloxane with parylene and its optimization, J. Micromech. Microeng. 21 (2011) 065024.

[136] M.A. Eddings, M.A. Johnson, B.K. Gale, Determining the optimal PDMS-PDMS bonding technique for microfluidic devices, J. Micromech. Microeng. 18 (2008) 067001.

[137] Y.-C. Tsai, N.-F. Chiu, P.-C. Liu, Y.-C. Ou, H.-H. Liao, Y.-J. Yang, L.-J. Yang, U. Lei, F.-S. Chao, S.-S. Lu, Fabrication process of integrated multi-analyte biochip system for implantable application, in: MEMS 2009 IEEE 22nd International Conference on Micro Electro Mechanical Systems, Sorrento, Italy, 2009, pp. 204–207.

[138] A. Khademhosseini, R. Langer, J. Borenstein, J.P. Vacanti, Microscale technologies for tissue engineering and biology, Proc. Nat. Acad. Sci. U.S.A. 103 (2006) 2480–2487.

[139] S.-R. Kim, A.I. Teixeira, P.F. Nealey, A.E. Wendt, N.L. Abbott, Fabrication of polymeric substrates with well-defined nanometer-scale topography and tailored surface chemistry, Adv. Mater. 14 (2002) 1468–1472.

[140] J. Jagur-Grodzinski, Polymers for tissue engineering, medical devices, and regenerative medicine. Concise general review of recent studies, Polym. Adv. Technol. 17 (2006) 395–418.

[141] T. Salo, K.-U. Kirstein, J. Sedivy, J. Grunenfelder, T. Vancura, G. Zund, H. Baltes, Continuous blood pressure monitoring utilizing a CMOS tactile sensor, in: IEMBS'04 26th Annual International Conference of the IEEE Engineering in Medicine and Biology Society, San Francisco, CA, USA, 2004, pp. 23226–23229.

[142] Institute for Polymers and Composites/I3N, Implantable Flexible Sensor Based on Aligned-Carbon Nanotubes for Blood Pressure Monitoring, Institute for Polymers and Composites/I3N, School of Engineering, University of Minho, 2011, www3.dsi.uminho.pt/seeum2011/cd/Posters/A591.pptx.

[143] M.B. Brown, G.P. Martin, S.A. Jones, F.K. Akomeah, Dermal and transdermal drug delivery systems: current and future prospects, Drug Delivery 13 (2006) 175–187.

[144] Y. Gao, T. Chen, X. Wang, J. Tang, Influence of hot embossed process parameters on biodegradable polymer microstructure for drug delivery, in: 2011 IEEE International Conference on Nano/Micro Engineered and Molecular Systems (NEMS), Kaohsiung, China, 2011, pp. 1246–1249.

[145] S. Adler, H.R. Brady, Cell adhesion molecules and the glomerulopathies, Am. J. Med. 107 (1999) 371–386.

[146] A. Sánchez, A.M. Álvarez, R. Pagan, C. Roncero, S. Vilaró, M. Benito, I. Fabregat, Fibronectin regulates morphology, cell organization and gene expression of rat fetal hepatocytes in primary culture, J. Hepatol. 32 (2000) 242–250.

[147] W.-I. Wu, K.N. Sask, J.L. Brash, P.R. Selvaganapathy, Polyurethane-based microfluidic devices for blood contacting applications, Lab Chip 12 (2012) 960–970.

[148] Nusil Silicone Technology, MED-1000 and MED-1011 Silicone Adhesives, Nusil Silicone Technology, 2005, http://www.silicone-polymers.com/pdf/MED-1000_1011P.PDF.

[149] H. Lee, J. Cho, Development of conformal PDMS and parylene coatings for microelectronics and MEMS packaging, in: 2005 ASME International Mechanical Engineering Congress and Exposition, Orlando, FL, USA, 2005, pp. 1–5.

[150] Y.S. Shin, K. Cho, S.H. Lim, S. Chung, S.-J. Park, C. Chung, D.-C. Han, J.K. Chang, PDMS-based micro PCR chip with parylene coating, J. Micromech. Microeng. 13 (2003) 768–774.

[151] N. Kawasaki, W.L. Kalb, T. Mathis, Y. Kaji, R. Mitsuhashi, H. Okamoto, Y. Sugawara, A. Fujiwara, Y. Kubozono, B. Batlogg, Flexible picene thin film field-effect transistors with parylene gate dielectric and their physical properties, Appl. Phys. Lett. 96 (2010) 113305.

[152] T.Y. Chang, V.G. Yadav, S. De Leo, A. Mohedas, B. Rajalingam, C.-L. Chen, S. Selvarasah, M.R. Dokmeci, A. Khademhosseini, Cell and protein compatibility of parylene-C surfaces, Langmuir 23 (2007) 11718–11725.

[153] W.F. Gorham, A new, general synthetic method for the preparation of linear poly-p-xylylenes, J. Polym. Sci., A: Polym. Chem. 4 (1966) 3027–3039.

[154] M. Gazicki-Lipman, Vapor deposition polymerization of para-xylylene derivatives-mechanism and applications, J. Vac. Soc. Jpn. 50 (2007) 601–608.

[155] A. Ramachandran, M. Junk, K.P. Koch, K.-P. Hoffmann, A study of parylene C polymer deposition inside microscale gaps, IEEE Trans. Adv. Packag. 30 (2007) 712–724.

[156] D.J. Broer, W. Luijks, Penetration of p-xylylene vapor into small channels prior to polymerization, J. Appl. Polym. Sci. 26 (1981) 2415–2422.

[157] G.E. Loeb, M.J. Bak, M. Salcman, E.M. Schmidt, Parylene as a chronically stable, reproducible microelectrode insulator, IEEE Trans. Biomed. Eng. (1977) 121–128.

[158] S. Kim, R. Bhandari, M. Klein, S. Negi, L. Rieth, P. Tathireddy, M. Toepper, H. Oppermann, F. Solzbacher, Integrated wireless neural interface based on the Utah electrode array, Biomed. Microdevices 11 (2009) 453–466.

[159] S. Takeuchi, D. Ziegler, Y. Yoshida, K. Mabuchi, T. Suzuki, Parylene flexible neural probes integrated with microfluidic channels, Lab Chip 5 (2005) 519–523.

[160] W. Li, D.C. Rodger, J.D. Weiland, M.S. Humayun, Y.C. Tai, Integrated flexible ocular coil for power and data transfer in retinal prostheses, in: IEEE-EMBS 2005 27th Annual International Conference of the Engineering in Medicine and Biology Society, Shanghai, China, 2006, pp. 1028–1031.

[161] D.C. Rodger, Y.-C. Tai, Microelectronic packaging for retinal prostheses, IEEE Eng. Med. Biol. Mag. 24 (2005) 52–57.

[162] A.J. Spence, K.B. Neeves, D. Murphy, S. Sponberg, B.R. Land, R.R. Hoy, M.S. Isaacson, Flexible multielectrodes can resolve multiple muscles in an insect appendage, J. Neurosci. Methods 159 (2007) 116–124.

[163] J.B. Fortin, T.-M. Lu, Chemical Vapor Deposition Polymerization: The Growth and Properties of Parylene Thin Films, Kluwer Academic Publisher, Dordrecht, The Netherlands, 2004.

[164] R. Kumar, D. Molin, L. Young, F. Ke, New high temperature polymer thin coating for power electronics, in: APEC'04 19th Annual IEEE Applied Power Electronics Conference and Exposition, Anaheim, CA, USA, 2004, pp. 1247–1249.

[165] J. Lahann, D. Klee, H. Höcker, Chemical vapour deposition polymerization of substituted [2.2]paracyclophanes, Macromol. Rapid Commun. 19 (1998) 441–444.

[166] J. Lahann, M. Balcells, H. Lu, T. Rodon, K.F. Jensen, R. Langer, Reactive polymer coatings: a first step toward surface engineering of microfluidic devices, Anal. Chem. 75 (2003) 2117–2122.

[167] J. Lahann, Reactive polymer coatings for biomimetic surface engineering, Chem. Eng. Commun. 193 (2006) 1457–1468.

[168] M.F. Nichols, Flexible and insulative plasmalene wire coatings for biomedical applications, Biomed. Sci. Instrum. 29 (1993) 77–86.

[169] J.J. Lentini, G.R. Severson, Humidity induced failures in parylene coated hybrids, Circuits Manuf. 21 (1984) 56–57.

[170] E.M. Schmidt, J.S. McIntosh, M.J. Bak, Long-term implants of parylene-C coated microelectrodes, Med. Biol. Eng. Comput. 26 (1988) 96–101.

[171] SCS, SCS Parylene Properties, 2007, http://www.physics.rutgers.edu/~podzorov/parylene%20properties.pdf.

[172] M.F. Nichols, The challenges for hermetic encapsulation of implanted devices—a review, CRC Crit. Rev. Bioeng. 22 (1994) 39–67.

[173] X. Wang, J. Engel, C. Liu, Liquid crystal polymer (LCP) for MEMS: processes and applications, J. Micromech. Microeng. 13 (2003) 628–633.

[174] T.F. Hayden, New liquid crystal polymer (LCP) flex circuits to meet demanding reliability and end-use applications requirements, in: 2002 International Conference on Advanced Packaging and Systems, Reno, NV, USA, 2002, pp. 116–122.

[175] E.C. Culbertson, A new laminate material for high performance PCBs: liquid crystal polymer copper clad films, in: Proceedings 45th Electronic Components and Technology Conference, Las Vegas, NV, USA, 1995, pp. 520–523.

[176] J. Jeong, S.W. Lee, K.S. Min, S.J. Kim, A novel multilayered planar coil based on biocompatible liquid crystal polymer for chronic implantation, Sens. Actuators, A: Phys. 197 (2013) 38–46.

[177] L. Frisk, E. Ristolainen, Flip chip attachment on flexible LCP substrate using an ACF, Microelectron. Reliab. 45 (2005) 583–588.

[178] A.-V. Pham, Packaging with liquid crystal polymer, IEEE Microwave Mag. 12 (2011) 83–91.

[179] D.C. Thompson, O. Tantot, H. Jallageas, G.E. Ponchak, M.M. Tentzeris, J. Papapolymerou, Characterization of liquid crystal polymer (LCP) material and transmission lines on LCP substrates from 30 to 110 GHz, IEEE Trans. Microwave Theory Tech. 52 (2004) 1343–1352.

[180] D.C. Thompson, M.M. Tentzeris, J. Papapolymerou, Packaging of MMICs in multilayer LCP substrates, IEEE Microwave Wireless Compon. Lett. 16 (2006) 410–412.

[181] T. Yoshikawa, Liquid crystal polymer (LCP) film "Vecstar", Electron. Parts Mater. 39 (2000) 42–46.

[182] F. Sunao, I. Hiroshi, Koumitsudo Kousyu-ha taiou kibanzairyou "BIAC", Electron. Parts Mater. (2002) 71–78.

[183] Inoue Hiroshi, Fukutake Sunao, H. Ohata, Liquid crystal polymer film with high heat resistance and high dimensional stability, in: SMTA'01 Sixth Pan Pacific Microelectronics Symposium, Kauai, Japan, 2001, pp. 273–278.

[184] R. Dean, J. Weller, M. Bozack, C. Farrell, L. Jauniskis, J. Ting, J. Edell, J. Hetke, Novel biomedical implant interconnects utilizing micromachined LCP, in: SPIE Nanoengineering: Fabrication, Properties, Optics, and Devices Conference, Denver, CO, USA, 2004, pp. 88–99.

[185] C.G.L. Khoo, B. Brox, R. Norrhede, F.H.J. Maurer, Effect of copper lamination on the rheological and copper adhesion properties of a thermotropic liquid

crystalline polymer used in PCB applications, IEEE Trans. Compon. Packag. Manuf. Technol., C 20 (1997) 219–226.

[186] K. Jayaraj, B. Farrell, Liquid crystal polymers and their role in electronic packaging, Adv. Microelectron. 25 (1998) 15–18.

[187] M.M.R. Howlader, M. Iwashita, K. Nanbu, K. Saijo, T. Suga, Enhanced Cu/LCP adhesion by pre-sputter cleaning prior to Cu deposition, IEEE Trans. Adv. Packag. 28 (2005) 495–502.

[188] B. Swinnen, W. Ruythooren, P. De Moor, L. Bogaerts, L. Carbonell, K. De Munck, B. Eyckens, S. Stoukatch, D.S. Tezcan, Z. Tokei, 3D integration by Cu–Cu thermo-compression bonding of extremely thinned bulk-Si die containing 10 μm pitch through-Si vias, in: IEDM'06 International Electron Devices Meeting, San Francisco, CA, USA, 2006, pp. 1–4.

[189] T. Yagihashi, Y. Wakabayashi, S. Fujita, Y. Fujita, M. Usui, Chalcosis bulbi recognized 22 years after trauma, Nippon Ganka Gakkai Zasshi 110 (2006) 990–994.

[190] S.W. Lee, J.-M. Seo, S. Ha, E.T. Kim, H. Chung, S.J. Kim, Development of microelectrode arrays for artificial retinal implants using liquid crystal polymers, Invest. Ophthalmol. Visual Sci. 50 (2009) 5859–5866.

[191] S.W. Lee, K.S. Min, J. Jeong, J. Kim, S.J. Kim, Monolithic encapsulation of implantable neuroprosthetic devices using liquid crystal polymers, IEEE Trans. Biomed. Eng. 58 (2011) 2255–2263.

[192] G. Fourche, An overview of the basic aspects of polymer adhesion. Part I: Fundamentals, Polym. Eng. Sci. 35 (1995) 957–967.

[193] A. Shigetou, T. Itoh, M. Matsuo, N. Hayasaka, K. Okumura, T. Suga, Bumpless interconnect through ultrafine Cu electrodes by means of surface-activated bonding (SAB) method, IEEE Trans. Adv. Packag. 29 (2006) 218–226.

[194] M.M.R. Howlader, F. Zhang, M.J. Deen, T. Suga, A. Yamauchi, Surface activated bonding of copper through silicon vias and gold stud bumps at room temperature, J. Vac. Sci. Technol., A 29 (2011) 021007.

[195] M.M.R. Howlader, A. Yamauchi, T. Suga, Surface activation-based nanobonding and interconnection at room temperature, J. Micromech. Microeng. 21 (2011) 025009.

[196] M.M.R. Howlader, T. Suga, A. Takahashi, K. Saijo, S. Ozawa, K. Nanbu, Surface activated bonding of LCP/Cu for electronic packaging, J. Mater. Sci. 40 (2005) 3177–3184.

[197] K. Nanbu, S. Ozawa, K. Yoshida, K. Saijo, T. Suga, Low temperature bonded Cu/LCP materials for FPCs and their characteristics, IEEE Trans. Compon. Packag. Technol. 28 (2005) 760–764.

[198] L. Chen, M. Crnic, Z. Lai, J. Liu, Process development and adhesion behavior of electroless copper on liquid crystal polymer (LCP) for electronic packaging application, IEEE Trans. Electron. Packag. Manuf. 25 (2002) 273–278.

[199] M. Zhou, W. Zhang, D. Ding, M. Li, The effect of pretreatment on adhesive strength of Cu-plated liquid crystal polymer (LCP), Appl. Surf. Sci. 258 (2012) 2643–2647.

[200] J. Ge, M.P.K. Turunen, J.K. Kivilahti, Surface modification of a liquid-crystalline polymer for copper metallization, J. Polym. Sci., B: Polym. Phys. 41 (2003) 623–636.

[201] D. Ha, W.N. de Vries, S.W.M. John, P.P. Irazoqui, W.J. Chappell, Polymer-based miniature flexible capacitive pressure sensor for intraocular pressure (IOP) monitoring inside a mouse eye, Biomed. Microdevices 14 (2012) 207–215.

[202] K. Hanseup, K. Najafi, Characterization of aligned wafer-level transfer of thin and flexible parylene membranes, J. Microelectromech. Syst. 16 (2007) 1386–1396.

[203] P.-J. Chen, W.-C. Kuo, W. Li, Y.-J. Yang, Y.-C. Tai, Q-enhanced fold-and-bond MEMS inductors, in: Third IEEE International Conference on Nano/Micro Engineered and Molecular Systems (NEMS), Sanya, China, 2008, pp. 869–872.

[204] L.P. Hromada, B.J. Nablo, J.J. Kasianowicz, M.A. Gaitan, D.L. DeVoe, Single molecule measurements within individual membrane-bound ion channels using a polymer-based bilayer lipid membrane chip, Lab Chip 8 (2008) 602–608.

[205] A. Taberham, M. Kraft, M. Mowlem, H. Morgan, The fabrication of lab-on-chip devices from fluoropolymers, J. Micromech. Microeng. 18 (2008) 064011.

[206] H.Y. Tan, W.K. Loke, Y.T. Tan, N.-T. Nguyen, A lab-on-a-chip for detection of nerve agent sarin in blood, Lab Chip 8 (2008) 885–891.

[207] J. Liu, S. Yang, C.S. Lee, D.L. DeVoe, Polyacrylamide gel plugs enabling 2-D microfluidic protein separations via isoelectric focusing and multiplexed sodium dodecyl sulfate gel electrophoresis, Electrophoresis 29 (2008) 2241–2250.

[208] Y. Wang, H. Chen, Q. He, S.A. Soper, A high-performance polycarbonate electrophoresis microchip with integrated three-electrode system for end-channel amperometric detection, Electrophoresis 29 (2008) 1881–1888.

[209] D.S.-W. Park, M.L. Hupert, M.A. Witek, B.H. You, P. Datta, J. Guy, J.-B. Lee, S.A. Soper, D.E. Nikitopoulos, M.C. Murphy, A titer plate-based polymer microfluidic platform for high throughput nucleic acid purification, Biomed. Microdevices 10 (2008) 21–33.

[210] Y.-X. Wang, Y. Zhou, B.M. Balgley, J.W. Cooper, C.S. Lee, D.L. DeVoe, Electrospray interfacing of polymer microfluidics to MALDI-MS, Electrophoresis 26 (2005) 3631–3640.

[211] Y. Li, J.S. Buch, F. Rosenberger, D.L. DeVoe, C.S. Lee, Integration of isoelectric focusing with parallel sodium dodecyl sulfate gel electrophoresis for multidimensional protein separations in a plastic microfludic network, Anal. Chem. 76 (2004) 742–748.

[212] T. Sultana, Bond quality and failure mode assessment for polymer-metal and polymer-glass transmission laser joints, in: Chemical Engineering, Wayne State University, Detroit, MI, USA, 2007.

[213] G.L. Georgiev, R.J. Baird, E.F. McCullen, G. Newaz, G. Auner, R. Patwa, H. Herfurth, Chemical bond formation during laser bonding of Teflon® FEP and titanium, Appl. Surf. Sci. 255 (2009) 7078–7083.

[214] A. Mian, T. Mahmood, G. Auner, R. Witte, H. Herfurth, G. Newaz, Effects of laser parameters on the mechanical response of laser irradiated micro-joints, Mater. Res. Soc. Symp. Proc. 926 (2006) 90–95.

[215] H. Liu, P. Li, A. Xing, Laser transmission welding of thermoplastic polyurethane films, Chin. J. Lasers 36 (2009) 156–160.

[216] X. Wang, P. Li, Z. Xu, X. Song, H. Liu, Laser transmission joint between PET and titanium for biomedical application, J. Mater. Process. Technol. 210 (2010) 1767–1771.

[217] G.L. Georgiev, T. Sultana, R.J. Baird, G. Auner, G. Newaz, R. Patwa, H. Herfurth, Laser bonding and characterization of Kapton® FN/Ti and Teflon® FEP/Ti systems, J. Mater. Sci. 44 (2009) 882–888.

[218] D.G. Georgiev, R.J. Baird, G. Newaz, G. Auner, R. Witte, H. Herfurth, An XPS study of laser-fabricated polyimide/titanium interfaces, Appl. Surf. Sci. 236 (2004) 71–76.

[219] A. Mian, G. Newaz, L. Vendra, N. Rahman, D.G. Georgiev, G. Auner, R. Witte, H. Herfurth, Laser bonded microjoints between titanium and polyimide for applications in medical implants, J. Mater. Sci.: Mater. Med. 16 (2005) 229–237.

[220] H. Potente, J. Korte, F. Becker, Laser transmission welding of thermoplastics: analysis of the heating phase, J. Reinf. Plast. Compos. 18 (1999) 914–920.

[221] T. Ebert, Keeping a clear view joining transparent plastics by laser, Kunstst.–Plast. Eur. 89 (1999) 17–18.

[222] J. Kim, X. Xu, Excimer laser fabrication of polymer microfluidic devices, J. Laser Appl. 15 (2003) 255–260.

[223] O. Rötting, W. Röpke, H. Becker, C. Gärtner, Polymer microfabrication technologies, Microsyst. Technol. 8 (2002) 32–36.

[224] H. Becker, C. Gärtner, Polymer microfabrication methods for microfluidic analytical applications, Electrophoresis 21 (2000) 12–26.

[225] P. Abgrall, C. Lattes, V. Conédéra, X. Dollat, S. Colin, A.M. Gué, A novel fabrication method of flexible and monolithic 3D microfluidic structures using lamination of SU-8 films, J. Micromech. Microeng. 16 (2006) 113–121.

[226] W.W. Chow, K.F. Lei, G. Shi, W.J. Li, Q. Huang, Microfluidic channel fabrication by PDMS-interface bonding, Smart Mater. Struct. 15 (2006) S112–S116.

[227] S. Lai, X. Cao, L.J. Lee, A packaging technique for polymer microfluidic platforms, Anal. Chem. 76 (2004) 1175–1183.

[228] C. Lu, L.J. Lee, Y.-J. Juang, Packaging of microfluidic chips via interstitial bonding technique, Electrophoresis 29 (2008) 1407–1414.

[229] B. Bilenberg, T. Nielsen, B. Clausen, A. Kristensen, PMMA to SU-8 bonding for polymer based lab-on-a-chip systems with integrated optics, J. Micromech. Microeng. 14 (2004) 814–822.

[230] G. Chen, J. Li, S. Qu, D. Chen, P. Yang, Low temperature bonding of poly(methylmethacrylate) electrophoresis microchips by in situ polymerisation, J. Chromatogr. A 1094 (2005) 138–147.

[231] J. Li, D. Chen, G. Chen, Low-temperature thermal bonding of PMMA microfluidic chips, Anal. Lett. 38 (2005) 1127–1136.

[232] G. Habenicht, Kleben: Grundlagen, Technologien, Anwendungen, Springer, Berlin, Germany, 2008.

[233] C.-W. Tsao, D.L. DeVoe, Bonding of thermoplastic polymer microfluidics, Microfluid. Nanofluid. 6 (2009) 1–16.

[234] R.T. Kelly, T. Pan, A.T. Woolley, Phase-changing sacrificial materials for solvent bonding of high-performance polymeric capillary electrophoresis microchips, Anal. Chem. 77 (2005) 3536–3541.

[235] X. Sun, B.A. Peeni, W. Yang, H.A. Becerril, A.T. Woolley, Rapid prototyping of poly(methyl methacrylate) microfluidic systems using solvent imprinting bonding, J. Chromatogr. A 1162 (2007) 162–166.

[236] H. Klank, J.P. Kutter, O. Geschke, CO₂-laser micromachining and back-end processing for rapid production of PMMA-based microfluidic systems, Lab Chip 2 (2002) 242–246.

[237] Y.C. Hsu, T.Y. Chen, Applying Taguchi methods for solvent-assisted PMMA bonding technique for static and dynamic micro-TAS devices, Biomed. Microdevices 9 (2007) 513–522.

[238] C.-H. Lin, C.-H. Chao, C.-W. Lan, Low azeotropic solvent for bonding of PMMA microfluidic devices, Sens. Actuators, B: Chem. 121 (2007) 698–705.

[239] F. Umbrecht, D. Müller, F. Gattiker, C. Boutry, J. Neuenschwander, U. Sennhauser, C. Hierold, Solvent assisted bonding of polymethylmethacrylate: characterization using the response surface methodology, Sens. Actuators, A: Phys. 156 (2009) 121–128.

[240] L. Brown, T. Koerner, J.H. Horton, R.D. Oleschuk, Fabrication and characterization of poly(methylmethacrylate) microfluidic devices bonded using surface modifications and solvents, Lab Chip 6 (2006) 66–73.

[241] M. Ohring, Materials Science of Thin Films, second ed., Academic Press, London, UK, 2001.

[242] M.J. Deen, The effect of the deposition rate on the properties of d.c.-magnetron-sputtered niobium nitride thin films, Thin Solid Films 152 (1987) 535–544.

[243] S. Mohtashami, M.M.R. Howlader, T. Doyle, Comparative electrochemical investigation of Pt, Au and Ti electrodes on liquid crystal polymer for the application of neuromuscular prostheses, ECS Trans. 35 (2011) 23–33.

[244] M.M.R. Howlader, T.E. Doyle, S. Mohtashami, J.R. Kish, Charge transfer and stability of implantable electrodes on flexible substrate, Sens. Actuators, B: Chem. 178 (2013) 132–139.

[245] K. Wang, C.-C. Liu, D.M. Durand, Flexible nerve stimulation electrode with iridium oxide sputtered on liquid crystal polymer, IEEE Trans. Biomed. Eng. 56 (2009) 6–14.

[246] Z.R. Huang, D. Guidotti, L. Wan, Y.-J. Chang, J. Yu, J. Liu, H.-F. Kuo, G.-K. Chang, F. Liu, R.R. Tummala, Hybrid integration of end-to-end optical interconnects on printed circuit boards, IEEE Trans. Compon. Packag. Technol. 30 (2007) 708–715.

[247] M.M.R. Howlader, F. Zhang, Void-free strong bonding of surface activated silicon wafers from room temperature to annealing at 600 °C, Thin Solid Films 519 (2010) 804–808.

[248] H. Takagi, R. Maeda, T. Suga, Transmission electron microscope observations of Si/Si interface bonded at room temperature by Ar beam surface activation, Jpn. J. Appl. Phys. 38 (1999) 1589–1594.

[249] H. Takagi, R. Maeda, T. Suga, Wafer-scale spontaneous bonding of silicon wafers by argon-beam surface activation at room temperature, Sens. Actuators, A: Phys. 105 (2003) 98–102.

[250] T. Yu, M.M.R. Howlader, F. Zhang, M. Bakr, Nanobonding for multi-junction solar cells at room temperature, ECS Trans. 35 (2011) 3–10.

[251] M.M.R. Howlader, T. Suga, F. Zhang, T.H. Lee, M.J. Kim, Interfacial behavior of surface activated p-GaP/n-GaAs bonded wafers at room temperature, Electrochem. Solid-State Lett. 13 (2010) H61–H65.

[252] M.M.R. Howlader, T. Watanabe, T. Suga, Investigation of the bonding strength and interface current of p-Si/n-GaAs wafers bonded by surface activated bonding at room temperature, J. Vac. Sci. Technol., B 19 (2001) 2114–2118.

[253] T.R. Chung, L. Yang, N. Hosoda, H. Takagi, T. Suga, Wafer direct bonding of compound semiconductors and silicon at room temperature by the surface activated bonding method, Appl. Surf. Sci. 117 (1997) 808–812.

[254] T. Mizumoto, H. Saito, K. Sakurai, Y. Shoji, Wafer bonding of magneto-optic garnet and its application to waveguide optical devices, ECS Trans. 3 (2007) 11–22.

[255] T. Mizumoto, H. Saito, Semi-leaky waveguide optical isolator, in: Optical Fiber Communication Conference, Anaheim, CA, U.S.A., 2007, pp. 1–3.

[256] Y. Shoji, T. Mizumoto, H. Yokoi, I.-W. Hsieh, R.M. Osgood, Magneto-optical isolator with silicon waveguides fabricated by direct bonding, Appl. Phys. Lett. 92 (2008) 071117.

[257] M.M.R. Howlader, T. Suga, M.J. Kim, A novel bonding method for ionic wafers, IEEE Trans. Adv. Packag. 30 (2007) 598–604.

[258] M.M.R. Howlader, H. Okada, T.H. Kim, T. Itoh, T. Suga, Wafer level surface activated bonding tool for MEMS packaging, J. Electrochem. Soc. 151 (2004) G461–G467.

[259] T. Suga, A. Takahashi, M. Howlader, K. Saijo, S. Oosawa, A lamination technique of LCP/Cu for electronic packaging, in: POLYTRONIC 2002 Second International IEEE Conference on Polymers and Adhesives in Microelectronics and Photonics, Zalaegerszeg, Hungary, 2002, pp. 177–182.

[260] M.M.R. Howlader, T.E. Doyle, Low temperature nanointegration for emerging biomedical applications, Microelectron. Reliab. 52 (2012) 361–374.

[261] M.M.R. Howlader, F. Zhang, M.G. Kibria, Void nucleation at a sequentially plasma-activated silicon/silicon bonded interface, J. Micromech. Microeng. 20 (2010) 065012.

[262] M.M.R. Howlader, M.G. Kibria, F. Zhang, M.J. Kim, Hybrid plasma bonding for void-free strong bonded interface of silicon/glass at 200 °C, Talanta 82 (2010) 508–515.

[263] M.M.R. Howlader, M.G. Kibria, F. Zhang, Hybrid plasma bonding of germanium and glass wafers at low temperature, Mater. Lett. 64 (2010) 1532–1535.

[264] A. Blau, Prospects for neuroprosthetics: flexible microelectrode arrays with polymer conductors, in: G.D. Gargiulo, A. McEwan (Eds.), Applied Biomedical Engineering, InTech, Rijeka, Croatia, 2011, pp. 83–122.

[265] M.S. Jones, D.S. Barth, Spatiotemporal organization of fast (>200 Hz) electrical oscillations in rat vibrissa/barrel cortex, J. Neurophysiol. 82 (1999) 1599–1609.

[266] M.M. El-Desouki, S.M. Abdelsayed, M.J. Deen, N.K. Nikolova, Y.M. Haddara, The impact of on-chip interconnections on CMOS RF integrated circuits, IEEE Trans. Electron Devices 56 (2009) 1882–1890.

[267] H.M. Jafari, M.J. Deen, S. Hranilovic, N.K. Nikolova, A study of ultrawideband antennas for near-field imaging, IEEE Trans. Antennas Propag. 55 (2007) 1184–1188.

[268] A. Baldi, W. Choi, B. Ziaie, A self-resonant frequency-modulated micromachined passive pressure transensor, IEEE Sens. J. 3 (2003) 728–733.

[269] A. DeHennis, K.D. Wise, A double-sided single-chip wireless pressure sensor, in: The 15th IEEE International Conference on Micro Electro Mechanical Systems, Las Vegas, NV, USA, 2002, pp. 252–255.

[270] O. Akar, T. Akin, K. Najafi, A wireless batch sealed absolute capacitive pressure sensor, Sens. Actuators, A: Phys. 95 (2001) 29–38.

[271] L. Rosengren, P. Rangsten, Y. Bäcklund, B. Hök, B. Svedbergh, G. Selén, A system for passive implantable pressure sensors, Sens. Actuators, A: Phys. 43 (1994) 55–58.

[272] M.A. Fonseca, M.G. Allen, J. Kroh, J. White, Flexible wireless passive pressure sensors for biomedical applications, in: Solid-State Sensor, Actuator, and Microsystems Workshop, Hilton Head Island, SC, USA, 2006, pp. 37–42.

[273] B.A. Hollenberg, C.D. Richards, R. Richards, D.F. Bahr, D.M. Rector, A MEMS fabricated flexible electrode array for recording surface field potentials, J. Neurosci. Methods 153 (2006) 147–153.

[274] J.D. Yeager, D.J. Phillips, D.M. Rector, D.F. Bahr, Characterization of flexible ECoG electrode arrays for chronic recording in awake rats, J. Neurosci. Methods 173 (2008) 279–285.

[275] P. Brunner, A.L. Ritaccio, T.M. Lynch, J.F. Emrich, J.A. Wilson, J.C. Williams, E.J. Aarnoutse, N.F. Ramsey, E.C. Leuthardt, H. Bischof, G. Schalk, A practical procedure for real-time functional mapping of eloquent cortex using electrocorticographic signals in humans, Epilepsy Behav. 15 (2009) 278–286.

[276] A. Gunduz, P. Brunner, A. Daitch, E.C. Leuthardt, A.L. Ritaccio, B. Pesaran, G. Schalk, Decoding covert spatial attention using electrocorticographic (ECoG) signals in humans, NeuroImage 60 (2012) 2285–2293.

[277] Z. Wang, A. Gunduz, P. Brunner, A.L. Ritaccio, Q. Ji, G. Schalk, Decoding onset and direction of movements using electrocorticographic (ECoG) signals in humans, Front. Neuroeng. 5 (2012) 15.

[278] A. Gunduz, P. Brunner, A. Daitch, E.C. Leuthardt, A.L. Ritaccio, B. Pesaran, G. Schalk, Neural correlates of visual-spatial attention in electrocorticographic signals in humans, Front. Hum. Neurosci. 5 (2011) 1–11.

[279] A.L. Ritaccio, Adventures in (subdural) space: high frequency EEG, the brain computer interface, and the new corticography, in: ASET 2010 Annual Conference, Louisville, KY, USA, 2011.

[280] B. Rubehn, C. Bosman, R. Oostenveld, P. Fries, T. Stieglitz, A MEMS-based flexible multichannel ECoG-electrode array, J. Neural Eng. 6 (2009) 036003.

[281] J. Viventi, D.-H. Kim, L. Vigeland, E.S. Frechette, J.A. Blanco, Y.-S. Kim, A.E. Avrin, V.R. Tiruvadi, S.-W. Hwang, A.C. Vanleer, Flexible, foldable, actively multiplexed, high-density electrode array for mapping brain activity in vivo, Nat. Neurosci. 14 (2011) 1599–1605.

[282] P.K. Campbell, K.E. Jones, R.J. Huber, K.W. Horch, R.A. Normann, A silicon-based, three-dimensional neural interface: manufacturing processes for an intracortical electrode array, IEEE Trans. Biomed. Eng. 38 (1991) 758–768.

[283] P.J. Rousche, D.S. Pellinen, D.P. Pivin Jr., J.C. Williams, R.J. Vetter, Flexible polyimide-based intracortical electrode arrays with bioactive capability, IEEE Trans. Biomed. Eng. 48 (2001) 361–371.

[284] V. Sankar, J.C. Sanchez, E. McCumiskey, N. Brown, C.R. Taylor, G.J. Ehlert, H.A. Sodano, T. Nishida, A highly compliant serpentine shaped polyimide interconnect for front-end strain relief in chronic neural implants, Front. Neurol. 4 (2013) 124.

[285] C. Henle, M. Raab, J.G. Cordeiro, S. Doostkam, A. Schulze-Bonhage, T. Stieglitz, J. Rickert, First long term in vivo study on subdurally implanted micro-ECoG electrodes, manufactured with a novel laser technology, Biomed. Microdevices 13 (2011) 59–68.

[286] C. Dupas-Bruzek, O. Robbe, A. Addad, S. Turrell, D. Derozier, Transformation of medical grade silicone rubber under Nd: YAG and excimer laser irradiation: first step towards a new miniaturized nerve electrode fabrication process, Appl. Surf. Sci. 255 (2009) 8715–8721.

[287] C. Dupas-Bruzek, P. Drean, D. Derozier, Pt metallization of laser transformed medical grade silicone rubber: last step toward a miniaturized nerve electrode fabrication process, J. Appl. Phys. 106 (2009) 074913.

[288] Z. Hu, D.M. Zhou, R. Greenberg, T. Thundat, Nanopowder molding method for creating implantable high-aspect-ratio electrodes on thin flexible substrates, Biomaterials 27 (2006) 2009–2017.

[289] M. David-Pur, L. Bareket-Keren, G. Beit-Yaakov, D. Raz-Prag, Y. Hanein, All-carbon-nanotube flexible multi-electrode array for neuronal recording and stimulation, Biomed. Microdevices (2013) 1–11.

[290] P. Kurian, B. Kasibhatla, J. Daum, C.A. Burns, M. Moosa, K.S. Rosenthal, J.P. Kennedy, Synthesis, permeability and biocompatibility of tricomponent membranes containing polyethylene glycol, polydimethylsiloxane and polypentamethylcyclopentasiloxane domains, Biomaterials 24 (2003) 3493–3503.

[291] A.R. Abate, D. Lee, T. Do, C. Holtze, D.A. Weitz, Glass coating for PDMS microfluidic channels by sol–gel methods, Lab Chip 8 (2008) 516–518.

[292] I. Pinnau, Z. He, Pure-and mixed-gas permeation properties of polydimethylsiloxane for hydrocarbon/methane and hydrocarbon/hydrogen separation, J. Membr. Sci. 244 (2004) 227–233.

[293] Z. Zhang, X. Feng, Q. Luo, B.-F. Liu, Environmentally friendly surface modification of PDMS using PEG polymer brush, Electrophoresis 30 (2009) 3174–3180.

[294] P. Ledochowitsch, E. Olivero, T. Blanche, M.M. Maharbiz, A transparent μECoG array for simultaneous recording and optogenetic stimulation, in: 2011 Annual International Conference of the IEEE Engineering in Medicine and Biology Society (EMBC), Boston, MA, USA, 2011, pp. 2937–2940.

[295] P. Ledochowitsch, R.J. Félus, R.R. Gibboni, A. Miyakawa, S. Bao, M.M. Maharbiz, Fabrication and testing of a large area, high density, parylene MEMS μECoG array, in: 2011 IEEE 24th International Conference on Micro Electro Mechanical Systems (MEMS), Cancun, Mexico, 2011, pp. 1031–1034.

[296] T. Bjorninen, R. Muller, P. Ledochowitsch, L. Sydanheimo, L. Ukkonen, M. Maharbiz, J. Rabaey, Design of wireless links to implanted brain–machine interface microelectronic systems, IEEE Antennas Wirel. Propag. Lett. 11 (2012) 1663–1666.

[297] D.C. Rodger, A.J. Fong, W. Li, H. Ameri, A.K. Ahuja, C. Gutierrez, I. Lavrov, H. Zhong, P.R. Menon, E. Meng, Flexible parylene-based multielectrode array technology for high-density neural stimulation and recording, Sens. Actuators, B: Chem. 132 (2008) 449–460.

[298] J.C.-H. Lin, Y. Zhao, P.-J. Chen, Y.-C. Tai, High quality factor parylene-based intraocular pressure sensor, in: 2012 Seventh IEEE International Conference on Nano/Micro Engineered and Molecular Systems (NEMS), Kyoto, Japan, 2012, pp. 137–140.

[299] P.-J. Chen, S. Saati, R. Varma, M.S. Humayun, Y.-C. Tai, Wireless intraocular pressure sensing using microfabricated minimally invasive flexible-coiled LC sensor implant, J. Microelectromech. Syst. 19 (2010) 721–734.

[300] C. Metallo, R.D. White, B.A. Trimmer, Flexible parylene-based microelectrode arrays for high resolution EMG recordings in freely moving small animals, J. Neurosci. Methods 195 (2011) 176–184.

[301] Y.-K. Song, W.R. Patterson, C.W. Bull, D.A. Borton, Y. Li, A.V. Nurmikko, J.D. Simeral, A brain implantable microsystem with hybrid RF/IR telemetry for advanced neuroengineering applications, in: EMBS 2007 29th Annual International Conference of the IEEE Engineering in Medicine and Biology Society, Lyon, France, 2007, pp. 445–448.

[302] J. Jeong, S.W. Lee, K. Min, K. Eom, S.H. Bae, S.J. Kim, Eye-surface conformable telemetric structure for polymer-based retinal prosthesis, in: 2011 Annual International Conference of the IEEE Engineering in Medicine and Biology Society, EMBC, Boston, MA, USA, 2011, pp. 1097–1100.

[303] R. Puers, G. Vandevoorde, D. De Bruyker, Electrodeposited copper inductors for intraocular pressure telemetry, J. Micromech. Microeng. 10 (2000) 124–129.

[304] W. Mokwa, U. Schnakenberg, Micro-transponder systems for medical applications, IEEE Trans. Instrum. Meas. 50 (2001) 1551–1555.

[305] Y. Bäcklund, L. Rosengren, B. Hök, B. Svedbergh, Passive silicon transensor intended for biomedical, remote pressure monitoring, Sens. Actuators, A: Phys. 21 (1990) 58–61.

[306] C.C. Collins, Miniature passive pressure transensor for implanting in the eye, IEEE Trans. Biomed. Eng. (1967) 74–83.

[307] B.B. Flick, R. Orglmeister, A portable microsystem-based telemetric pressure and temperature measurement unit, IEEE Trans. Biomed. Eng. 47 (2000) 12–16.

[308] T. Eggers, J. Draeger, K. Hille, C. Marschner, P. Stegmaier, J. Binder, R. Laur, Wireless intra-ocular pressure monitoring system integrated into an artificial lens, in: First Annual International Conference on Microtechnologies in Medicine and Biology, Lyon, France, 2000, pp. 466–469.

[309] EggersF T., C. Marschner, U. Marschner, B. Clasbrummel, R. Laur, J. Binder, Advanced hybrid integrated low-power telemetric pressure monitoring system for biomedical applications, in: The 13th Annual International Conference on Micro Electro Mechanical Systems, MEMS 2000, Miyazaki, Japan, 2000, pp. 329–334.

[310] A.S. Walton, H. Krum, The heartpod implantable heart failure therapy system, Heart, Lung Circ. 14 (2005) S31–S33.

[311] S.H. Ellozy, A. Carroccio, R.A. Lookstein, T.S. Jacobs, M.D. Addis, V.J. Teodorescu, M.L. Marin, Abdominal aortic aneurysm sac shrinkage after endovascular aneurysm repair: correlation with chronic sac pressure measurement, J. Vasc. Surg. 43 (2006) 2–7.

[312] S.H. Ellozy, A. Carroccio, R.A. Lookstein, M.E. Minor, C.M. Sheahan, J. Juta, A. Cha, R. Valenzuela, M.D. Addis, T.S. Jacobs, First experience in human beings with a permanently implantable intrasac pressure transducer for monitoring endovascular repair of abdominal aortic aneurysms, J. Vasc. Surg. 40 (2004) 405–412.

[313] B. Puers, W. Sansen, R. Vereecken, Development considerations of a micropower control chip and ultraminiature hybrid for bladder pressure telemetry, in: Biotelemetry VIII: The Eighth International Symposium on Biotelemetry, Dubrovnik, Yugoslavia, 1984, pp. 328–332.

[314] E. Siwapornsathain, A. Lal, J. Binard, A telemetry and sensor platform for ambulatory urodynamics, in: Second Annual International IEEE-EMB Special Topic Conference on Microtechnologies in Medicine & Biology, Madison, WI, USA, 2002, pp. 283–287.

[315] G.S. Wilson, M.A. Johnson, *In-vivo* electrochemistry: what can we learn about living systems? Chem. Rev. 108 (2008) 2462–2481.

[316] S.J. Martin, V.E. Granstaff, G.C. Frye, Characterization of a quartz crystal microbalance with simultaneous mass and liquid loading, Anal. Chem. 63 (1991) 2272–2281.

[317] J.S. Alpert, The Heart Attack Handbook, Little, Brown & Company, Boston, MA, USA, 1978.

[318] X. Li, T. Reissman, F. Yu, E.C. Kan, A low-range drift-free bio-compatible pressure sensor based on P(VDF-TrFE) piezoelectric thin film, in: Mater. Res. Soc. Symp. Proc, Boston, MA, USA, 2009, p. 1222.

[319] Y. Lee, S. Bae, H. Jang, S. Jang, S.-E. Zhu, S.H. Sim, Y.I. Song, B.H. Hong, J.-H. Ahn, Wafer-scale synthesis and transfer of graphene films, Nano Lett. 10 (2010) 490–493.

[320] R.L. Parker, A. Krinsky, Electrical resistance-strain characteristics of thin evaporated metal films, J. Appl. Phys. 34 (1963) 2700–2708.

[321] S. Ullerich, W. Mokwa, G. Vom Bogel, U. Schnakenberg, Micro coils for an advanced system for measuring intraocular pressure, in: First Annual International Conference on Microtechnologies in Medicine and Biology, Lyon, France, 2000, pp. 470–474.

[322] U. Schnakenberg, P. Walter, G. Vom Bögel, C. Krüger, H.C. Lüdtke-Handjery, H.A. Richter, W. Specht, P. Ruokonen, W. Mokwa, Initial investigations on systems for measuring intraocular pressure, Sens. Actuators, A: Phys. 85 (2000) 287–291.

[323] K. Stangel, S. Kolnsberg, D. Hammerschmidt, B.J. Hosticka, H.K. Trieu, W. Mokwa, A programmable intraocular CMOS pressure sensor system implant, IEEE J. Solid-State Circuits 36 (2001) 1094–1100.

[324] W. Mokwa, Ophthalmic implants, in: Proceedings IEEE Sensors Conference, Toronto, Canada, 2003, pp. 980–986.

[325] K. Min, J.Y. Jung, T.H. Han, Y. Park, C. Jung, S.M. Hong, C.M. Koo, Graphene electrodes for artificial muscles, Mol. Cryst. Liq. Cryst. 539 (2011) 260–265.

[326] X. Liu, Y. Zhu, M.W. Nomani, X. Wen, T.-Y. Hsia, G. Koley, A highly sensitive pressure sensor using a Au-patterned polydimethylsiloxane membrane for biosensing applications, J. Micromech. Microeng. 23 (2013) 025022.

[327] D.A. Gough, L.S. Kumosa, T.L. Routh, J.T. Lin, J.Y. Lucisano, Function of an implanted tissue glucose sensor for more than 1 year in animals, Sci. Transl. Med. 2 (2010) 1–8.

[328] D.J. Macaya, M. Nikolou, S. Takamatsu, J.T. Mabeck, R.M. Owens, G.G. Malliaras, Simple glucose sensors with micromolar sensitivity based on organic electrochemical transistors, Sens. Actuators, B: Chem. 123 (2007) 374–378.

[329] D.A. Chang-Yen, B.K. Gale, Integrated optical glucose sensor fabricated using PDMS waveguides on a PDMS substrate, in: SPIE Microfluidics, BioMEMS, and Medical Microsystems Conference, San Jose, CA, USA, 2004, pp. 98–107.

[330] Y.J. Heo, S. Takeuchi, Towards smart tattoos: implantable biosensors for continuous glucose monitoring, Adv. Healthcare Mater. 2 (2013) 43–56.

[331] G. Jiang, Design challenges of implantable pressure monitoring system, Front. Neurosci. 4 (2010) 1–4.

[332] E.M. Yeatman, D. O'Hare, C. Dobson, E. Bitziou, Approaches to self-powered biochemical sensors for *in-vivo* applications, in: Proceedings of the ICST 3rd International Conference on Body Area Networks, Brussels, Belgium, 2008, pp. 15–16.

[333] O. Secchi, M. Zinellu, Y. Spissu, M. Pirisinu, G. Bazzu, R. Migheli, M.S. Desole, R.D. O'Neill, P.A. Serra, G. Rocchitta, Further *in-vitro* characterization of an implantable biosensor for ethanol monitoring in the brain, Sensors 13 (2013) 9522–9535.

[334] J. Wang, S. Chan, R.R. Carlson, Y. Luo, G. Ge, R.S. Ries, J.R. Heath, H.-R. Tseng, Electrochemically fabricated polyaniline nanoframework electrode junctions that function as resistive sensors, Nano Lett. 4 (2004) 1693–1697.

[335] C. García-Aljaro, M.A. Bangar, E. Baldrich, F.J. Muñoz, A. Mulchandani, Conducting polymer nanowire-based chemiresistive biosensor for the detection of bacterial spores, Biosens. Bioelectron. 25 (2010) 2309–2312.

[336] W.H. Ko, Early history and challenges of implantable electronics, ACM J. Emerg. Technol Comput. Syst. 8 (2012) 8.

[337] S. Zhang, F. Awaja, N. James, D.R. McKenzie, A.J. Ruys, Autohesion of plasma treated semi-crystalline PEEK: comparative study of argon, nitrogen and oxygen treatments, Colloids Surf., A: Physicochem. Eng. Aspects 374 (2011) 88–95.

[338] F. Awaja, S. Zhang, N. James, D.R. McKenzie, Free radicals generated by ion bombardment of a semi-crystalline PEEK surface, Plasma Processes Polym. 9 (2012) 174–179.

[339] F. Awaja, S. Zhang, N. James, D.R. McKenzie, Plasma activation and self bonding of PEEK for the use in the encapsulation of medical implants, Plasma Processes Polym. 7 (2010) 866–875.

[340] A.D. DeHennis, K.D. Wise, A fully integrated multisite pressure sensor for wireless arterial flow characterization, J. Microelectromech. Syst. 15 (2006) 678–685.

[341] J.A. Potkay, Long term, implantable blood pressure monitoring systems, Biomed. Microdevices 10 (2008) 379–392.

[342] N. Winkin, W. Mokwa, Flexible multi-electrode array with integrated bendable CMOS-chip for implantable systems, in: 2012 Annual International Conference of the IEEE Engineering in Medicine and Biology Society (EMBC), San Diego, CA, USA, 2012, pp. 3882–3885.

[343] H. Yu, N. Zheng, W. Wang, S. Wang, X. Zheng, Z. Li, Electroplated nickel multielectrode microprobes with flexible parylene cable for neural recording and stimulation, J. Microelectromech. Syst. 22 (2013) 1199–1206.

[344] Y. Onuki, U. Bhardwaj, F. Papadimitrakopoulos, D.J. Burgess, A review of the biocompatibility of implantable devices: current challenges to overcome foreign body response, J. Diabetes Sci. Technol. 2 (2008) 1003–1015.

[345] M. Waleed Shinwari, M. Jamal Deen, D. Landheer, Study of the electrolyte-insulator-semiconductor field-effect transistor (EISFET) with applications in biosensor design, Microelectron. Reliab. 47 (2007) 2025–2057.

[346] M.W. Shinwari, D. Zhitomirsky, I.A. Deen, P.R. Selvaganapathy, M.J. Deen, D. Landheer, Microfabricated reference electrodes and their biosensing applications, Sensors 10 (2010) 1679–1715.

[347] B. Yu, C. Wang, Y.M. Ju, L. West, J. Harmon, Y. Moussy, F. Moussy, Use of hydrogel coating to improve the performance of implanted glucose sensors, Biosens. Bioelectron. 23 (2008) 1278–1284.

[348] C.P. Quinn, C.P. Pathak, A. Heller, J.A. Hubbell, Photo-crosslinked copolymers of 2-hydroxyethyl methacrylate, poly(ethylene glycol) tetra-acrylate and ethylene dimethacrylate for improving biocompatibility of biosensors, Biomaterials 16 (1995) 389–396.

[349] I. Galeska, T.-K. Kim, S.D. Patil, U. Bhardwaj, D. Chattopadhyay, F. Papadimitrakopoulos, D.J. Burgess, Controlled release of dexamethasone from PLGA microspheres embedded within polyacid-containing PVA hydrogels, AAPS J. 7 (2005) E231–E240.

[350] C. Espadas-Torre, M.E. Meyerhoff, Thrombogenic properties of untreated and poly(ethylene oxide)-modified polymeric matrixes useful for preparing intraarterial ion-selective electrodes, Anal. Chem. 67 (1995) 3108–3114.

[351] G.P. Rigby, S. Ahmed, G. Horseman, P. Vadgama, *In vivo* glucose monitoring with open microflow-influences of fluid composition and preliminary evaluation in man, Anal. Chim. Acta 385 (1999) 23–32.

[352] C.A.P. Quinn, R.E. Connor, A. Heller, Biocompatible, glucose-permeable hydrogel for *in situ* coating of implantable biosensors, Biomaterials 18 (1997) 1665–1670.

[353] K. Paralikar, P. Cong, O. Yizhar, L.E. Fenno, W. Santa, C. Nielsen, D. Dinsmoor, B. Hocken, G.O. Munns, J. Giftakis, An implantable optical stimulation delivery system for actuating an excitable biosubstrate, IEEE J. Solid-State Circuits 46 (2011) 321–332.

[354] D.R. Merrill, M. Bikson, J.G.R. Jefferys, Electrical stimulation of excitable tissue: design of efficacious and safe protocols, J. Neurosci. Methods 141 (2005) 171–198.

[355] M. Kfouri, O. Marinov, P. Quevedo, N. Faramarzpour, S. Shirani, L.W.-C. Liu, Q. Fang, M.J. Deen, Toward a miniaturized wireless fluorescence-based diagnostic imaging system, IEEE J. Sel. Top. Quantum Electron. 14 (2008) 226–234.

[356] S. Steudel, S. De Vusser, S. De Jonge, D. Janssen, S. Verlaak, J. Genoe, P. Heremans, Influence of the dielectric roughness on the performance of pentacene transistors, Appl. Phys. Lett. 85 (2004) 4400–4402.

[357] W.-Y. Lin, R. Müller, K. Myny, S. Steudel, J. Genoe, P. Heremans, Room-temperature solution-processed high-k gate dielectrics for large area electronics applications, Org. Electron. 12 (2011) 955–960.

[358] Y. Qin, D.H. Turkenburg, I. Barbu, W.T.T. Smaal, K. Myny, W.-Y. Lin, G.H. Gelinck, P. Heremans, J. Liu, E.R. Meinders, Organic thin-film transistors with anodized gate dielectric patterned by self-aligned embossing on flexible substrates, Adv. Funct. Mater. 22 (2012) 1209–1214.

[359] T. Sugiyama, Y. Iimori, K. Baba, M. Watanabe, H. Honma, Surface metallization on high temperature liquid-crystal-polymer film by UV-irradiation process, J. Electrochem. Soc. 156 (2009) D360–D363.

[360] C. Yang, K. Shin, S.Y. Yang, H. Jeon, D. Choi, D.S. Chung, C.E. Park, Low-voltage organic transistors on a polymer substrate with an aluminum foil gate fabricated by a laminating and electropolishing process, Appl. Phys. Lett. 89 (2006) 153508.

[361] N. Lago, K. Yoshida, K.P. Koch, X. Navarro, Assessment of biocompatibility of chronically implanted polyimide and platinum intrafascicular electrodes, IEEE Trans. Biomed. Eng. 54 (2007) 281–290.

[362] K.-K. Lee, J. He, A. Singh, S. Massia, G. Ehteshami, B. Kim, G. Raupp, Polyimide-based intracortical neural implant with improved structural stiffness, J. Micromech. Microeng. 14 (2004) 32–37.

[363] Dupont Kapton Polyimide Film General Specifications, Bulletin GS-96-7, Dupont Kapton Polyimide Film General Specifications, 2012, http://www2.dupont.com/Kapton/en_US/assets/downloads/pdf/Gen_Specs.pdf.

[364] K. Lee, A. Singh, J. He, S. Massia, B. Kim, G. Raupp, Polyimide based neural implants with stiffness improvement, Sens. Actuators, B: Chem. 102 (2004) 67–72.

[365] B.-E. El Mohajir, N. Heymans, Changes in structural and mechanical behaviour of PVDF with processing and thermomechanical treatments. 1. Change in structure, Polymer 42 (2001) 5661–5667.

[366] D.J. Hourston, I.D. Hughes, Poly(vinylidene fluoride)-poly(methyl methacrylate) blends, Polymer 18 (1977) 1175–1178.

[367] Quadrant Engineering Plastic Products, Product Data Sheet, SYMALIT® PVDF 1000, Quadrant Engineering Plastic Products, 2007, http://www.quadrantplastics.com/fileadmin/quadrant/documents/QEPP/EU/Product_Data_Sheets_PDF/Symalit/Symalit_PVDFFlex1000_E_PDS_0907.pdf.

[368] Polyflon, PVDF Fluoropolymer Film, Polyflon, 2011, http://www.polyflon.co.uk/datasheets/pvdf_film.pdf.

[369] T. Sakakibara, H. Izu, T. Kura, W. Shinohara, H. Iwata, S. Kiyama, Development of high-voltage photovoltaic micro-devices for an energy supply to micro-machines, in: Fifth International Symposium on Micro Machine and Human Science, Nagoya, Japan, 1994, pp. 71–76.

[370] Measurement Specialties, Inc., Piezo Film Sensors Technical Manual, 2012, http://meas-spec.com/downloads/Piezo_Technical_Manual.pdf.

[371] R.K. Goyal, A.N. Tiwari, U.P. Mulik, Y.S. Negi, Thermal expansion behaviour of high performance PEEK matrix composites, J. Phys. D: Appl. Phys. 41 (2008) 085403.

[372] A.K. van der Vegt, L.E. Govaert, Polymeren: van keten tot kunststof, DUP Blue Print, Delft, The Netherlands, 2003.

[373] J. Pan, K. Li, J. Li, T. Hsu, Q. Wang, Dielectric characteristics of poly(ether ketone ketone) for high temperature capacitive energy storage, Appl. Phys. Lett. 95 (2009) 022902.

[374] N. Amanat, C. Chaminade, J. Grace, D.R. McKenzie, N.L. James, Transmission laser welding of amorphous and semi-crystalline poly-ether-ether-ketone for applications in the medical device industry, Mater. Des. 31 (2010) 4823–4830.

[375] T.W. Odom, J.C. Love, D.B. Wolfe, K.E. Paul, G.M. Whitesides, Improved pattern transfer in soft lithography using composite stamps, Langmuir 18 (2002) 5314–5320.

[376] B.-B. Li, Q.-Y. Wang, Y.-F. Xiao, X.-F. Jiang, Y. Li, L. Xiao, Q. Gong, On chip, high-sensitivity thermal sensor based on high-Q polydimethylsiloxane-coated microresonator, Appl. Phys. Lett. 96 (2010) 251109.

[377] B.-B. Li, Q.-Y. Wang, X.-F. Jiang, Q. Gong, Y.-F. Xiao, High-sensitivity temperature sensing by employing an on-chip high-Q PDMS-coated toroidal microcavity, in: SPIE Photonic Microdevices/Microstructures for Sensing III Conference, Orlando, FL, USA, 2011, p. 80340J.

[378] N. Bowden, W.T.S. Huck, K.E. Paul, G.M. Whitesides, The controlled formation of ordered, sinusoidal structures by plasma oxidation of an elastomeric polymer, Appl. Phys. Lett. 75 (1999) 2557–2559.

[379] H. van der Werff, A.J. Pennings, High strength and high modulus fibers of poly(p-xylylene), Polym. Bull. 19 (1988) 587–594.

[380] J.J. Senkevich, S.B. Desu, Morphology of poly(chloro-p-xylylene) CVD thin films, Polymer 40 (1999) 5751–5759.

[381] B.-K. Chen, S.-Y. Tsay, J.-Y. Chen, Synthesis and properties of liquid crystalline polymers with low T_m and broad mesophase temperature ranges, Polymer 46 (2005) 8624–8633.

[382] C.J. Lee, S.J. Oh, J.K. Song, S.J. Kim, Neural signal recording using microelectrode arrays fabricated on liquid crystal polymer material, Mater. Sci. Eng., C 24 (2004) 265–268.

[383] S.E. Lee, S.B. Jun, H.J. Lee, J. Kim, S.W. Lee, C. Im, H.-C. Shin, J.W. Chang, S.J. Kim, A flexible depth probe using liquid crystal polymer, IEEE Trans. Biomed. Eng. 59 (2012) 2085–2094.

[384] S. Kärki, J. Lekkala, A new method to measure heart rate with EMFi and PVDF materials, J. Med. Eng. Technol. 33 (2009) 551–558.

[385] F. Awaja, S. Zhang, N. James, D.R. McKenzie, Enhanced autohesive bonding of polyetheretherketone (PEEK) for biomedical applications using a methane-oxygen plasma treatment, Plasma Processes Polym. 7 (2010) 1010–1021.

[386] E.Y. Chow, A.L. Chlebowski, P.P. Irazoqui, A miniature-implantable RF-wireless active glaucoma intraocular pressure monitor, IEEE Trans. Biomed. Circuits Syst. 4 (2010) 340–349.

Biographies

Yiheng Qin is currently pursuing a Ph.D. degree in Department of Electrical and Computer Engineering at McMaster University, Hamilton, Canada. He received his B.S. degree in Electronics Science and Technology (Microelectronics Technology) from Southwest Jiaotong University, Chengdu, China, in 2009, and received his M.S. degree in Microtechnology from Chalmers University of Technology, Göteborg, Sweden, in 2011. His research interests include nano-integration technologies, with a focus on the use of polymeric materials in nano-scaled bonding and integration for biomedical and environmental applications.

Matiar M.R. Howlader received a B.Sc. Eng. degree in Electrical and Electronic Engineering from Khulna University of Engineering and Technology, in Khulna, Bangladesh, in 1988, and his M.S. and Ph.D. degrees in Nuclear Engineering from Kyushu University, Fukuoka, Japan, in 1996 and 1999, respectively. Currently, Dr. Howlader is leading the nanobonding and packaging research group in the Department of Electrical and Computer Engineering at McMaster University, Hamilton, ON, Canada. His research focuses on the nano-integration of bio-micro-opto-electromechanical systems and implantable systems for health and environmental applications.

M. Jamal Deen received the Ph.D. degree in electrical engineering and applied physics from Case Western Reserve University, Cleveland, OH, in 1985. His Ph.D. dissertation was focused on the design and modeling of a new CARS spectrometer for dynamic temperature measurements and combustion optimization in rocket and jet engines, and was sponsored and used by NASA, Cleveland. He is currently a Professor of Electrical and Computer Engineering, Senior Canada Research Chair in Information Technology and Director of the Micro- and Nano-Systems Laboratory at McMaster University. His research interests include nanoelectronics, optoelectronics, and nanotechnology and their emerging applications for health and environmental sciences.

Yaser M. Haddara received the B.Eng. degree in electrical engineering from the Memorial University of Newfoundland, St. John's, NB, Canada, in 1991, and the M.S. and Ph.D. degrees from Stanford University, Stanford, CA, USA, in 1993 and 1997, respectively. He was a Postdoctoral Research Associate with the University of Florida, Gainesville, USA, and a Senior Engineer in the device group with Cypress Semiconductor. Since 2002, he has been with McMaster University, Hamilton, ON, Canada, where he is currently an Associate Professor of Electrical and Computer Engineering. His research interests are in front-end silicon and silicon-germanium process modeling, technology CAD, polymer semiconductor devices and processing, and RF circuit design.

P. Ravi Selvaganapathy received the B.S. degree in chemical and electrochemical engineering from Central ElectroChemical Research Institute, Karaikudi, India, in 1998, and the M.S. and Ph.D. degrees in electrical engineering and computer science from the University of Michigan, Ann Arbor, USA, in 2001 and 2002, respectively. He was engaged in various projects related to MEMS and BioMEMS processes and device development including electrochemical detection in capillary electrophoresis systems, electroosmotic pumping systems, thermal phase-change polymers, porous polymers in microsystems, and investigation of microplasmas as a fluorescence excitation source for DNA. From 2003 to 2004, he was a Postdoctoral Research Associate at Bionano Systems, Division of Sandia National Laboratories, Livermore, CA, USA, where he is engaged for the development of an integrated sensing system for low-concentration protein detection with biodefense applications. He is currently an Associate Professor in Department of Mechanical Engineering, McMaster University, Hamilton, ON, Canada.